# Developing an in Vivo Based CRISPR-Induced Genetic Screen to Identify Novel Regulators of T-Cell Dysfunction in the Context of Tumors

# Developing an *in vivo* Based CRISPR-Induced Genetic Screen to Identify Novel Regulators of T-cell Dysfunction in the Context of Tumors

Justin D. Trombley

A Thesis in the Field of Biology

for the Degree of Master of Liberal Arts in Extension Studies

Harvard University

November 2018

## Abstract

T-cell dysfunction is a central characteristic of the immune system's response to cancer, and one of the primary mechanisms that allows tumors to escape the immune response and thrive. Within the last decade, there has been rapid progress in immunotherapy treatments that are capable of manipulating the immune system to target and attack cancer cells. Two immunotherapy treatments in particular, antibody checkpoint blockade and chimeric antigen receptor (CAR) modified T-cells, have been especially effective in preventing or reversing T-cell dysfunction in the context of tumors. However, these immunotherapies are not without their limitations, as only certain subsets of patients have robust responses to these treatments and many show no response at all. It is therefore imperative that we discover novel therapeutic targets of T-cell dysfunction in the context of tumors, and this can best be achieved through large-scale loss-of-function genetic screens. The efficiency and affordability of the recently developed CRISPR-Cas9 genomic DNA editing technology makes it an ideal method for performing large scale genetic screens. The primary goal of this thesis was to develop the tools necessary to create an *in vivo* based CRISPR-mediated system that could be used to generate a genetic screen to discover novel negative regulators of T-cell dysfunction in the tumor microenvironment. Targets discovered in such a screen will be useful to identify novel therapeutic targets for use in both checkpoint blockade and CAR T-cell therapies.

Acknowledgments

First and foremost, I would like to thank Dr. Sharpe, my thesis director, without whom this would not have been possible. You have supported and encouraged me throughout my thesis project, and for that I am grateful. I would also like to thank Martin LaFleur, whose scientific and technical advice has been invaluable. You have made me a better scientist.

I would also like to thank my family and friends. You all provided encouragement and distraction when I needed it most. Finally, I would like to especially thank Dr. Christina Reppucci. You never doubted me and I would not be here without you.

Table of Contents

List of Tables

List of Figures

# Chapter I.

# Introduction

## Cancer Immunotherapy Background

The idea that the immune system is vital in killing aberrantly transformed cells before they develop into tumors originated with Paul Ehrlich in the early 20th century (Ehrlich 1909). This hypothesis remained controversial for decades. Initially, it was unclear whether tumors expressed specific and distinct antigens that could be recognized and targeted by the immune system. If there were no antigens specific to tumors, then it would be impossible for the immune system to distinguish tumors from normal host tissue and thus the immune system would be unable to target and kill the tumors without damaging the host. As the field of immunology matured and tumor associated antigens were discovered experimentally, Ehrlich's initial hypothesis was further developed and expanded upon, eventually becoming known as the cancer immunosurveillance hypothesis (Burnet 1957).

The cancer immune surveillance model, however, failed to gain widespread acceptance after experiments with athymic, immunocompromised nude mice showed no more susceptibility than healthy mice at developing chemically induced or spontaneous tumors (Stutman, 1974; Stutman, 1979). This research strongly suggested that the immune system had minimal effect on the controlling and killing of tumors, leading to the abandonment of the cancer immunosurveillance hypothesis (Dunn, Bruce, Ikeda, Old, & Schreiber, 2002). However, it was later found that the nude mice were less

immunocompromised than previously thought (Ikehara, Pahwa, Fernandes, Hansen, & Good, 1984), and likely did have adaptive immune protection from tumor formation. This unknown caveat set back tumor immunology research by decades.

Interest in the cancer immunosurveillance hypothesis was gradually renewed after a series of experiments in the 1990s showed that immunocompromised mice, developed through the knockout of genes important for immune cell function, were more susceptible to both spontaneous and induced tumors (Dunn et al., 2002; Kim, Emi, & Tanabe, 2007). However, while it became accepted that the immune system is capable of finding and killing tumor cells once they are transformed, it also became clear that the immune surveillance theory was incomplete. If the immune system is capable of controlling tumor cells, then tumors should only form and grow in immunocompromised individuals, but they also form in immunologically healthy individuals. This apparent paradox was eventually elucidated by Shankaran et al. (2001), who found that not only does the immune system protect against cancer development, but it also selects for tumor cells with reduced immunogenicity. In other words, the immune system helps to create tumor cells that are capable of avoiding immune surveillance and can eventually develop into malignant cancer. This led to the more nuanced cancer immunoediting hypothesis, which incorporated the immune system's complex role of both host-protection and tumor-sculpting actions (Dunn et al., 2002).

Of particular interest in cancer immunology is the interaction between T-cells and tumors, as T-cells are the major driving force of the adaptive immune system. Tumor cells can express ligands that bind to T-cell inhibitory receptors, known as checkpoints, that downregulate the T-cell response and prevent T-cell activation (Baumeister,

Freeman, Dranoff, & Sharpe, 2016). Under normal circumstances these inhibitory receptors prevent autoimmunity and promote self tolerance. However, persistent exposure to these inhibitory signals eventually leads to T-cell dysfunction, where the effector function is lost (Jiang and Zhu, 2015). T-cell dysfunction is a central characteristic of the immune system's response to cancer, and one of the primary mechanisms that allows tumors to escape the immune response and thrive.

Within the last decade, there has been rapid progress in clinical research on immunotherapies that focus on the treatment of cancer. Whereas classical treatments like chemotherapy or radiation kill tumor cells directly, immunotherapies instead trigger or enhance immune cell function which in turn controls and kills the tumor cells. Two forms of cancer immunotherapy in particular have been shown to be effective tumor therapies: 1) antibody checkpoint blockade and 2) chimeric antigen receptor (CAR) modified T-cells (Ribas & Wolchok, 2018). Checkpoint blockade involves the use of monoclonal antibodies that "block" the binding of negative immune regulators by tumors, which can ultimately reverse T-cell dysfunction and allow for better tumor killing function (Pardoll, 2012). CAR T-cells, on the other hand, are T-cells that have been engineered to both specifically kill tumors as well as be hyper activated through strong costimulatory domains encoded within the modified receptors (Lee et al. 2012).

While these immunotherapies are very promising, they are not without their flaws. Only certain subsets of patients have robust responses to these treatments, and many show no response at all (Kvistborg & Yewdell, 2018; Ribas & Wolchok, 2018). Additionally, adverse side effects, including death in some cases, remain a risk with these immunotherapies (Hodi et al., 2010; Hartmann, Schüßler-Lenz, Bondanza, & Buchholz,

2017). The emergence of the CRISPR (clustered regularly interspaced short palindromic repeats)/Cas (CRISPR-associated) DNA editing systems in mammalian cells (Cong et al., 2013) has provided the means for both improving the efficacy and safety of current immunotherapy treatments, as well as discovering novel regulators of T-cell dysfunction. Such discoveries could act as potential new targets for immunotherapies that may offer more effective and/or safer treatments.

## T-cell Development and Dysfunction

T-cells are the primary drivers of the adaptive immune system, and one of the main areas of focus in cancer immunology research. Unlike the innate immune system, which is a generalized first-line of defense, the T-cell response in the adaptive immune system is uniquely specific to foreign or tumor-associated antigen peptides. They can largely be broken up into two major types: helper T-cells and cytotoxic T-cells, which are distinguishable based on the cell-surface expression of either CD4 (helper T-cells) or CD8 (cytotoxic T-cells) glycoprotein (Germain, 2002). Helper T-cells are important in "helping" the maturation or activation of other immune cell types to facilitate an immune response, while cytotoxic T-cells seek out and kill infected or malignant cells directly.

In the naïve state, $CD8^+$ T-cells are fully mature but cannot perform effector functions (e.g., cytotoxic activity, cytokine production) until activation. T-cell activation begins after a T-cell receptor (TCR) binds to its cognate antigen peptide presented by an innate immune cell (e.g., dendritic cell, macrophage), referred to as an antigen presenting cell (APC) (Smith-Garvin, Koretzky, & Jordan, 2009). Importantly, activation also requires engagement of co-stimulatory receptors on the naïve T-cell, such as CD28, by

B7 proteins expressed by an APC. Only after receiving both signals will a naïve T-cell undergo activation, which causes the T-cell to acquire effector functions and proliferate to deal with a given threat (Chen & Flies, 2013). Most, but not all, effector T-cells eventually die off shortly after the threat has been cleared, a process known as contraction. However, a small portion of these cells survive to differentiate into memory T-cells (Germain, 2002). Memory T-cells provide long term immunity as they "remember" the antigen in case the threat recurs; if memory T-cells are exposed to a similar antigen again, they are more capable than naïve/effector T-cells at expanding and responding to the threat.

In addition to co-stimulatory receptors, activated T-cells express co-inhibitory receptors. If during antigen presentation a naïve T-cell also receives a co-inhibitory signal from the APC, the T-cell response will be downregulated (Chen & Flies, 2013). These inhibitory receptors are known as checkpoints, and like the co-stimulatory molecules are mediated through the engagement of T-cell receptors by ligands on the APC. These checkpoints ensure that T-cells only become activated when necessary, thus promoting tolerance of the self and preventing autoimmunity. Some of the co-inhibitory receptors expressed on T-cells include PD-1 (programmed cell death protein 1) and CTLA-4 (cytotoxic T-lymphocyte -associated antigen 4), as well as TIM-3 (T-cell immunoglobulin domain and mucin domain protein 3), LAG-3 (lymphocyte activation gene 3 protein), and TIGIT (T-cell immunoreceptor with Ig and ITIM domains) (Chen & Flies, 2013).

Since cancer cells are derived from normal host tissue, they are often capable of exploiting mechanisms that evolved to prevent self-recognition and autoimmunity. By

overexpressing ligands of inhibitory receptor checkpoints, like PD-1 and CTLA-4, cancer cells can suppress $CD8^+$ T-cell activation. Persistent exposure to tumor antigens accompanied by chronic signaling through co-inhibitory receptors eventually causes the cytotoxic T-cells to become dysfunctional and lose effector function, allowing the tumor to escape the immune response and thrive (Jiang and Zhu, 2015). Recently, however, advances in cancer immunology research have shown that cytotoxic T-cell dysfunction in the context of tumors can be reversed through what is known as checkpoint blockade.

## Checkpoint Blockade

Treatments that manipulate the immune system to target and attack cancer cells, known as cancer immunotherapy, have created a paradigm shift in how medical science approaches cancer treatments. Checkpoint blockade in particular has been incredibly influential, and it was among the first kind of immunotherapies approved by the US Food and Drug Association (FDA) for the treatment of cancer (Cameron, Whiteside, & Perry, 2011). The idea behind checkpoint blockade is that negative regulators of immune cells are overexpressed by tumors and prevent the immune system from attacking and clearing tumors as they develop. Monoclonal antibodies that "block" the engagement of inhibitory receptors on tumor infiltrating lymphocytes (TILs), such as T-cells, are capable of temporarily reversing T-cell dysfunction and restoring effector function, thus allowing the TILs to attack and kill tumor cells (Sakuishi et al., 2010).

The concept of checkpoint blockade as a treatment for cancer originated with a study in 1996 that found that injecting tumor-bearing mice with a monoclonal antibody that blocks engagement of CTLA-4 with B7 ligands resulted in the inhibition or rejection

of tumors (Leach, Krummel, & Allison, 1996). CTLA-4 is a negative regulator of T-cells and was the first immune checkpoint to be extensively studied in cancer immunotherapy research (Cameron, Whiteside, & Perry, 2011). It inhibits T-cell activation by preventing engagement of the co-stimulatory receptor CD28 by competing with the B7 ligands expressed by dendritic cells (Pentcheva-Hoang, Egen, Wojnoonski, & Allison, 2004). The binding of CTLA-4 with B7 ligands causes T-cells to become anergic, and perpetual engagement eventually leads to dysfunction (Allison, 1994). Thus, blocking the ability of B7 ligands to bind with CTLA-4 prevented and/or reversed T-cell dysfunction, allowing for a sustained immune response which resulted in attenuated tumor growth.

While research performed with mouse models is often not translatable to humans, a phase 3 clinical trial testing ipilimumab, a monoclonal antibody that blocks engagement of CTLA-4 with its ligands, has been shown to shrink tumors and demonstrated a survival benefit to a subset of patients with advanced melanoma (Hodi et al., 2010). A year later, ipilimumab was approved by the FDA for the treatment of melanoma ("FDA Approval for Ipilimumab," 2011). However, CTLA-4 blockade is not without its limitations. So far no other cancers have been approved by the FDA for CTLA-4 antibody blockade treatment alone. Additionally, only a subset of patients responded to the ipilimumab treatment in the clinical study, and serious adverse events occurred as a result of the treatment, including death of 2.1% of the patients (Hodi et al., 2010).

Antibodies that target the inhibitory receptor PD-1 and its ligand, PD-L1, have shown greater promise in treating a wider variety of cancers compared to CTLA-4 blockade; tumor regressions have been observed in clinical studies using PD-1 blockade for melanoma, colon, renal, and lung cancers (Pardoll, 2012). This is because many

tumors express PD-L1 (Kleffel et al., 2015; Bhaijee & Anders, 2016; Gupta et al., 2016; Juneja et al., 2017) which binds to PD-1 on $CD8^+$ T-cells and results in their deactivation within the tumor microenvironment. In fact, expression of PD-L1 by the tumors is likely an adaptive response to anti-tumor immunity, as tumor expression of PD-L1 increases after T-cells infiltrate the tumors (Taube et al., 2013).

While PD-1 blockade has shown great promise, a majority of patients do not respond to treatment (Tang et al., 2016). This is likely because PD-1 blockade alone is not enough to completely reverse T-cell dysfunction within the context of tumors, however, PD-1 in combination with other checkpoint blocking antibodies appears to be more effective. Combined PD-1 and CTLA-4 blockade has been found to be more effective in the treatment of variety of cancers in tumor-bearing mice than either treatment alone (Selby et al., 2016). There have also been clinical studies that found the combined treatment of PD-1 and CTLA-4 blocking antibodies in melanoma and in renal cell carcinoma showed improved response rates compared to either antibody alone (Larkin, Hodi, & Wolchok; 2015; Postow et al., 2015; Hammers et al., 2017).

While PD-1 and CTLA-4 are the only co-inhibitory targets approved by the FDA for oncology treatments, Tim-3, Lag-3 and TIGIT make up the next wave of co-inhibitory targets that are currently undergoing clinical trials (Anderson, Joller, & Kuchroo, 2016). These immune receptors are all similar to PD-1 and CTLA-4, but each regulates T-cell response to cancer uniquely. If these drugs are approved, it will likely allow for a greater variety of combinations for more targeted immunotherapy treatments. Nevertheless, it is still important to research and discover potential novel targets for checkpoint blockade, as this would allow for an even greater variety of combinational

therapies that could potentially lead to better response rates with fewer side effects. Using a genetic-based screen has the potential to find novel checkpoint regulators and novel combination therapies that may be useful for future checkpoint blockade oncology treatments.

## CAR T-cell Therapy

For decades immunologists debated over whether tumor cells express antigens that differ from normal cells, thus allowing for an immune response, or simply overexpress normal proteins that would lead to self tolerance (Dunn et al., 2002). While research has shown that cancer cells can express unique antigens that are immunogenic (Sahin et al., 1995), most T-cells with high affinity TCRs to tumor antigens are eliminated during development (Kim & Ahmed, 2010). This is to prevent self-recognition and autoimmunity, however it allows for greater chance of immunological escape by tumors. One potential approach to improve anti-tumor immunity is to genetically engineer a cancer patient's own T-cells with modified TCRs that are better able to bind to and kill tumor cells. This approach is known as CAR T-cell immunotherapy.

CAR T-cell therapy works by collecting T-cells from the blood of cancer patients and then modifying the TCRs so that they have greater affinity to antigen(s) expressed by the patient's tumor. These cells are then expanded in culture and then adoptively transferred back into the patients, where the modified T-cells are more capable of seeking out and attacking the tumors than unmodified T-cells (Lee et al., 2012). CAR T-cells can also be modified to downregulate expression of checkpoint inhibitors, such as PD-1 or CTLA-4, in order to prevent the T-cells from undergoing dysfunction and further

enhance their tumor killing abilities. Whereas monoclonal antibody checkpoint blockade is more generalized and can alter the entire immune system, CAR T-cells have arguably greater therapeutic potential due to the possibility of more personalized therapies. CAR T-cells have the potential to be engineered to attack tumors that are normally resistant to checkpoint blocking antibodies.

Despite their potential, CAR T-cell therapies are not without their limitations. So far only two CAR T-cell therapies have been approved by the by the FDA ("FDA Approves," 2017), and both are only for the treatment of B-cell hematologic tumors. While these CAR T-cell therapies have been extremely successful in treating those cancers, it also affected non-cancerous B-cells and resulted in an almost complete depletion of patients' B-cell repertoire (D'Aloia, Zizzari, Sacchetti, Pierelli, & Alimandi, 2018). Fortunately, as D'Aloia et al. (2018) point out, B-cell depletion can be tolerated by patients with immunoglobulin treatment, however this may not be true for other cell lineages. Additionally, some patients infused with CAR T-cells in clinical trials for B-cell hematologic tumors experienced severe side effects such as hypoxia or neurological disturbances that required intensive medical care (Davila et al., 2014). This was a result of a systemic inflammatory response caused by a large-scale release of cytokines from on-target CAR T-cells.

Even more problematic, however, is that CAR T-cell therapy has been ineffective in treating solid tumors, such as those in colon, breasts, or lung, due to T-cell suppression and insufficient T-cell localization to the tumors (Yong et al., 2017). A variety of concepts are currently being explored to overcome these barriers, such as ways to improve localization of CAR T-cells to the site of the tumor or improve infiltration into

the tumor once CAR T-cells are there (Hu, 2017; Yong et al., 2017). The identification of novel T-cell checkpoint regulators could help CAR T-cells overcome such obstacles, as it could lead the creation of a variety of modified T-cells more resistant to dysfunction and suppression. A genetic-based screen utilizing CRISPR-Cas9 has the potential find such novel checkpoint regulators.

## CRISPR-Cas9 Genetic Modifications

In order to understand how and why the immune system fails in the context of tumors, it is imperative that we identity genes that negatively regulate immune cells and prevent them from clearing the tumors. This can best be achieved by large-scale loss-of-function genetic screens, which allow for the identification of the function of many genes at once. However, while genetic screens have been very successful for single-celled organisms, the diploid nature of mammalian cells has made screens considerably more difficult to perform since it requires inactivation of both copies of a gene (Wang, Wei, Sabatini, & Lander, 2014).

There are DNA editing technologies that allow for disruption of both alleles, such as zinc finger nucleases (ZFN) or transcription activator-like effector nucleases (TALEN), however performing large-scale genomic screens has been limited due to the high costs, low efficiency, and length of time needed to perform the editing using these methods (Hsu, Lander, & Zhang, 2014). One commonly employed workaround is the use of RNA interference (RNAi), where instead of knocking out the gene, the production of the associated protein is disrupted by interfering with the translation of the mRNA (Ngo

et al., 2006). However this solution too is imperfect due to its off-target effects and incomplete suppression of targeted genes (Boutros & Ahringer, 2008).

The emergence of the CRISPR-Cas9 genomic DNA editing systems allows researchers to edit genomes by adding, altering, or removing specific DNA sequences in a way that is much easier and cheaper than previous genomic DNA editing systems (Cong et al., 2013; Hsu, Lander, & Zhang, 2014). Originally discovered in bacteria, this biological system has since been co-opted and engineered for genome editing of human cells, rodents, and many other types of organisms. There are two key components to the CRISPR-Cas9 system: a Cas9 protein and a single chimeric guide RNA (sgRNA). Cas9 is an enzyme that can cut double stranded DNA at a specific location in the genome, and this allows for altering of the genome. The sgRNA is a short strand of RNA complexed with the Cas9 protein that can bind to a specific complementary DNA sequence within the genome, which directs the Cas9 to a specific location within the genome to cut. Researchers can then use endogenous DNA repair components to modify the DNA through the removal or insertion of DNA sequences (Hsu, Lander, & Zhang, 2014)

The sgRNA is what distinguishes the CRISPR-Cas9 system from other genomic editing methods, such as ZFN or TALENs which use proteins to target DNA sites (Gaj, Gersbach, & Barbas, 2013). With CRISPR, all that is needed to target a variety of DNA motifs is to modify a small target site-specific sequence at the 5′ end of the sgRNA, whereas ZFN or TALENs require researchers to painstakingly engineer a custom protein for each new gene target (Boettcher & McManus, 2015). The ease of engineering and the affordability of modifying the sgRNA sequences make the CRISPR-Cas9 system ideal for performing large-scale genetic screens. Such a screen could be used on $CD8^+$ T-cells

to identify novel therapeutic targets for use in both checkpoint blockade and CAR T-cell therapies.

In addition identifying novel regulators of T-cells through loss-of-function screens of individual genes, CRISPR-Cas9 can be used to perturb multiple genes within the same genome to discover interactions between genes (Wong et al., 2016). Sometimes perturbing two genes simultaneously can lead to unexpected phenotypic consequences when considering the effect of each individual mutation (Mani, St.Onge, Hartman, Giaever, & Roth, 2008). It is already known that combining different forms of checkpoint blockade can yield improved responses in the context of cancers. In some patients with untreated melanoma for example, combination of PD-1 and CTLA-4 blockade has been shown to be more effective than either treatment alone (Larkin, Hodi, & Wolchok, 2015). Any novel regulators of T-cell dysfunction discovered during a targeted CRISPR-mediated screen could then be used in a combinatorial screen with each other or with already known checkpoint inhibitors. This would have the potential to discover novel combinations in the clinical setting with improved treatment responses, which is especially important in cancer immunotherapy where only a subset of patients respond to treatments.

## Research Approach, Goals, and Hypotheses

The primary goal of this thesis was to develop the tools necessary to create an *in vivo* based CRISPR-mediated system that could be used to generate a genetic screen to discover novel negative regulators of T-cell dysfunction in the tumor microenvironment. Previous *in vivo* based screens looking for immunotherapy targets in the contexts of

tumors used RNAi to knockdown the genes (Zhou et al., 2014), however this approach suffers from incomplete suppression of the genes (Boutros & Ahringer, 2008). A CRISPR-based screen, on the other hand, results in a complete knockout of genes and thus a complete loss of function.

We determined that developing this system would be best achieved by refining our methods and tools using a checkpoint inhibitor already established to be important in preventing or reversing T-cell dysfunction in the context of tumors. For this reason, the PD-1 was chosen as an ideal target as it meets these criteria for both animal research and clinical trials. Replicating the known protective effects of PD-1 blockade on T-cell function in the tumor microenvironment would serve as confirmation that our assays and methods were effective. To further evaluate the efficacy of our manipulations, we performed *in vivo* T-cell competitive assays, which involves the adoptive transfer of two different $CD8^+$ T-cell types into tumor-bearing mice to determine which is enriched (i.e., which has a competitive advantage) within the tumor microenvironment. The aggressive B16 mouse melanoma was chosen as our tumor model as it is used for pre-clinical studies and is difficult to treat (Hosoi et al., 2014). While it is sensitive to PD-1 blockade and PD-1 deficient immune cells, clearance of tumors only occurs when it is paired with another treatment (Juneja et al., 2017). This should allow enough time to complete the competitive assays before the tumors are cleared.

In Experiment 1 we established an *in vivo* competitive assay in the B16 tumor microenvironment using T-cells from conventional PD-1 knockout ($PD\text{-}1^{KO}$) mice. This was completed by adoptively transferring $CD8^+$ T-cells from $PD\text{-}1^{KO}$ and wild-type (WT) mice in equal proportion into mice induced with tumors. We hypothesized that 8 days

after the adoptive transfer there would be a greater proportion of the PD-1 KO T-cells isolated from the tumor and draining inguinal lymph node (dLN) relative to the WT T-cells, but no significant difference in T-cell origin in the spleen or irrelevant brachial lymph node (iLN).

In Experiment 2 we repeated the process outlined for Experiment 1 above, but used CRISPR-Cas9 mediated PD-1 deficient T-cells instead of cells T-cells isolated from conventional PD-$1^{KO}$ mice. This was done in order to verify that T-cells with CRISPR-mediated deletion of the PD-1 gene, *Pdcd1*, would perform functionally similar to conventional PD-$1^{KO}$ T-cells. We hypothesized we would replicate the findings from Experiment 1, finding a greater proportion of PD-1 deficient T-cells compared to WT T-cells in the tumor and draining lymph node 8 days after the adoptive transfer.

In addition to the CRISPR-mediated single target loss-of-function screens, we wanted to establish that the CRISPR-Cas9 system could be used to perturb multiple genes within the same genome; thus allowing discovery of interactions between genes. As a proof of concept, in Experiment 3 we used a CRISPR-Cas9 vector and two sgRNAs to simultaneously knockout two different genes in vitro. Specifically, we aimed to knock-out both *Pdcd1* and *Ptpn2* (Tyrosine-protein phosphatase non-receptor type 2). *Ptpn2* was chosen as the second target due to its role in self-tolerance and preventing autoimmunity (Wiede, Gruta, & Tiganis, 2014), and as such it could potentially improve $CD8^+$ T-cell response in the tumor microenvironment. We hypothesized we would be able to successfully knockout *Pdcd1* and *Ptpn2* in the same cells using the CRISPR-Cas9 system.

Finally, we wanted modify the constitutively expressing CRISPR-Cas9 vector used in Experiments 2 and 3 to make an inducible CRISPR-Cas9 vector utilizing the CreER$^{T2}$-lox system. In Experiment 4, we disrupted transcription of the tracrRNA of the CRISPR-Cas9 vector by inserting a transcription terminator sequence flanked by loxP sites within the tracrRNA sequence. We also inserted a tamoxifen-dependent Cre recombinase, known as Cre-ER$^{T2}$ downstream of the tracrRNA sequence in the vector. Thus, only in the presence of 4-OHT (4-hydroxytamoxifen) will Cre recombinase be transcribed and translated, leading to excision of the transcription terminator sequence within the tracrRNA sequence. We hypothesized that we would successfully create an inducible CRISPR-Cas9 system by adding this CreER$^{T2}$-lox system into the constitutive CRISPR-Cas9 vector.

At the completion of this thesis project, we aim to have 1) established an *in vivo* competitive assay of T-cell function in the context of tumors, 2) verified the efficacy of CRISPR-mediated gene deletion in T-cells, 3) confirmed the feasibility of using the CRISPR-Cas9 system for the simultaneous deletion of two genes within the same genome, and 4) created an inducible CRISPR-Cas9 vector. Together, the experiments in this project will have made substantial progress toward the goal of developing the tools necessary to create an *in vivo* based CRISPR-mediated genetic screening system able discover novel negative regulators of T-cell dysfunction in the tumor microenvironment.

# Chapter II.

# Materials and Methods

## Cell Line Culturing

HEK-293x cells, ovalbumin-expressing B16 (B16-OVA) cells, and Cas9-expressing B16 (B16-Cas9) cells were grown in a humidified atmosphere incubator (Heraeus) at 37°C and 5% CO2. The cells were cultured in Dulbecco's modified eagle medium (DMEM) supplemented with 10% fetal bovine serum (FBS, Sigma), 1% penicillin/streptomycin (Gibco), and 20 μg/ml gentamicin (Gibco). B16-OVA cell lines were generated by transducing B16 cells with the lentiviral TRC-pLX305 vector containing ovalbumin protein and a gene for puromycin resistance (Broad Institute). Two days before tumor injections, the puromycin-resistant B16-OVA cells were cultured with 2 μg/ml of puromycin for selection. B16-Cas9 cells were originally created by Manguso et. al (2017)

## Guide Design and Cloning

The sgRNA oligonucleotides were designed based on the CRISPR algorithm provided by the Broad Institute (Table 1) (Doench et al., 2016). Using BsmBI restriction digestion enzymes, the sgRNAs were then cloned into a constitutive sgRNA vector that had been modified from a lentiviral shRNA vector (Godec et al., 2015) to express the Vex (violet-excited-fluorescent GFP) (Anderson M.T. et al., 1998) or RFP (red fluorescent protein) fluorophore. Four different sgRNA vectors were produced: 1) $Vex^{+}$

vector with a *Ptpn2* targeting sgRNA, 2) $Vex^{+}$ non-targeting sgRNA control vector, 3) $RFP^{+}$ vector with a *Pdcd1* targeting sgRNA, and 4) $RFP^{+}$ non-targeting sgRNA control vector.

Additionally, for Experiment 4, the constitutive sgRNA vector was modified to be an inducible sgRNA vector through the insertion of the ligand (4-OHT-dependent $CRE\text{-}ER^{T2}$ (Ruzankina et al., 2007) and a transcriptional stop codon flanked by loxP sites (loxP-Stop-loxP) within the tracrRNA sequence. This was done using gBlocks Gene Fragments obtained from IDT.

## Lentivirus Production and Titering

Lentivirus was generated by transfecting HEK-293X cells with one of the sgRNA vectors described above along with the helper plasmids Pspax2 and Md2g (provided by Dr. Cigall Kadoch, Dana Farber Cancer Institute). The transfections were carried out using polyethylenimine (PEI) at a ratio of 30 (PEI): 4 (sgRNA oligonucleotide): 10 (Pspax2): 1 (Md2g) in mixed in Optimem (Gibco) in complete DMEM. After 72 h, the supernatants containing the virus were syringe-filtered at 30 μm and then centrifuged at 20,000 g for 2 h. The supernatant was then carefully removed and allowed to dry for 3-5 min, after which the viral pellets were carefully resuspended in media, covered, and incubated on ice overnight at 4°C.

To quantify the viral load, a viral titer was performed by transducing the HEK-293X cells with the concentrated virus. The cells were seeded at 25,000 cells per well in 200 μl in a 96-well flat bottom plate (Falcon) and transduced using polybrene at 10

μg/mL with serial dilutions of concentrated virus. The media was changed 24 h after transduction, and analyzed via flow cytometry on a Cytoflex (Beckman Coulter). The transduction units per mL (TU/mL), where each unit represents one lentiviral particle, were calculated based on the percent $Vex^+$ or $RFP^+$.

## B16-Cas9 and HEK-293x Cell Line Transduction

In a 6-well plate (BD Falcon), 200,000 B16-Cas9 tumor cells were cultured in 2 mL of complete DMEM. After 24 h (and 1 h prior to transduction), the media was changed. Each well was polybrene transduced (1 μg/mL, Santa Cruz) with two sgRNA vectors, where one vector expressed Vex and the other expressed RFP. There were 4 groups: 1) $Vex^+$ *Ptpn2* sgRNA and $Vex^+$ CTL-1 sgRNA, 2) $RFP^+$ *Pdcd1* sgRNA and $RFP^+$ CTL-2 sgRNA, 3) $RFP^+$ *Pdcd1* sgRNA and $Vex^+$ *Ptpn2*, and 4) $Vex^+$ Control-1 sgRNA and $RFP^+$ Control-2 sgRNA

After 24 h, media was changed. The transduced cells were then cultured for a total of 10 days to allow for complete CRISPR-editing, with puromycin (2 μg/ml) added for the final 3 days to select for B16-Cas9 cells. On day 10, the cells were stained with 7-AAD, sorted ($7\text{-}AAD^-$, $Vex^+$, $RFP^+$), and then used in the TIDE Assay.

The HEK-293x cell line was transduced with the Cre-$ER^{T2}$ vector using the methods described above. The cells were then collected for flow cytometry to determine transduction efficiency based on Vex expression, and to determine Cre expression by way of an intracellular stain using a primary anti-Cre recombinase antibody raised in rabbit (Abcam) and a phycoerythrin (PE)-conjugated donkey anti-rabbit IgG secondary antibody (BioLegend).

## TIDE Assay

Tracking of Indels by Decomposition (TIDE) assay was used to determine DNA knockout efficiency in transduced B16-Cas9 cells, as previously described (Brinkman, Chen, Amendola, & van Steensel, 2014). After transduced cells were sorted, the DNA was extracted using a Blood and Tissue DNAeasy Kit (Qiagen) and then amplified via PCR). PCR products were then purified using the PCR Purification Kit (Qiagen) and then submitted to the DF/HCC DNA Sequencing Facility for Sanger sequencing. Table 2 contains all TIDE primers for sequencing.

## Animals

C57BL/6J CD45.2 $^{+}$ recipient mice for adoptive transfers were obtained from Jackson Laboratories at 6 weeks of age. Upon arrival, subjects were allowed at least 1 week to acclimate to the colony room. All other experimental mice were generated on-site by the Sharpe laboratory. OT-I mice (C57BL/6-Tg(TcraTcrb)1100Mjb/J) and CD45.1 mice (B6.SJL-Ptprca Pepcb/BoyJ) were originally obtained from Jackson laboratories. PD-1$^{KO}$ (*Pdcd1*$^{-/-}$) mice were created in the Sharpe laboratory (Keir, Freeman, & Sharpe, 2007). Loxp-stop-loxp Cas9 knockin mice were a gift from Dr. Feng Zhang, Massachusetts Institute of Technology (Platt et al. 2014) and then modified by breeding them to Zp3-Cre mice (C57BL/6-Tg(Zp3-cre)1Gwh/J) from Jackson Laboratories (LaFleur et al. 2018). These various mouse lines were bred to generate the five types of donor mice used for adoptive T-cell transfers: OT-I$^{+}$ CD45.1$^{+}$ WT, OT-I$^{+}$

CD45.1/CD45.2$^{+}$ WT, OT-I$^{+}$ CD45.1/CD45.2$^{+}$ PD-1$^{KO}$, OT-I$^{+}$ Cas9 CD45.2$^{+}$, and OT-I$^{+}$ Cas9 CD45.1/45.2$^{+}$.

All mice were maintained in the same animal facility at Harvard Medical School. Mice were group-housed, maintained on a 12-h light/dark cycle, and had access to food and water ad libitum. All housing and experimental procedures were in compliance with the National Institutes of Health Guidelines for Care and Use of Laboratory Animals, and approved by the Harvard Medical School Institutional Animal Care and Use Committee.

## Tumor Model

C57BL/6J CD45.2$^{+}$ mice (7 weeks old) were anesthetized with Avertin (2.5% 2,2,2-Tribromoethanol) and then injected subcutaneously in the flank with 2.0 x 106 B16 tumor cells expressing ovalbumin (B16-OVA). Tumors were measured every 48-72 h with digital calipers. The formula of an ellipsoid was used to determine tumor volume: ½ x D x d2, where D is the major axis and d is the minor axis.

## Adoptive T-cell Transfers

T-cells with the transgenic OT-I T-cell receptor, which is specific to the antigen OVA expressed by the B16-OVA tumor cell line (Hogquist et al., 1994), were used for all adoptive transfer experiments. In Experiment 1, naive CD8$^{+}$ T-cells were purified using a naïve CD8$^{+}$ MACS kit (Miltenyi Biotec) from 6-10 week old OT-I$^{+}$ CD45.1$^{+}$ WT mice and from conventional OT-I$^{+}$ CD45.1/CD45.2$^{+}$ PD-1$^{KO}$ mice. To control for the effect of stimulation and transduction of the T-cells performed in Experiment 2, in

Experiment 1 a mock transduction (Zhou et al. 2014) was performed on the T-cells before being adoptively transferred into B16-OVA tumor-bearing mice. First, the OT-I$^{+}$ CD8$^{+}$ T-cells were cultured in Roswell Park Memorial Institute media (RPMI 1640, Gibco) supplemented with FBS (10%), 2-mercaptoethanol (0.05mM, Sigma), penicillin-streptomycin (1%), and HEPES (20 mM, Gibco), and then stimulated with IL-7 (5 ng/mL, Peprotech) and IL-15 (100 ng/mL, Peprotech). After 48 h, the T-cells were placed in a 24-well plate (BD Falcon) coated with retronectin (5μg/mL, Takara), supplemented with protamine sulfate (5μg/mL, EMD Millipore), and spun at 800 g at 37°C for 1 h in order to simulate the spin-infection

Following the spin, the T-cells were cultured in 24-well plates in complete RPMI media (Gibco), stimulated with IL-7 (2.5 ng/mL), IL-15 (50 ng/mL) and IL-2 (100 units/mL, Peprotech). After an additional 72 h, PD-1$^{KO}$ and WT T-cells were then stained with lineage fluorescently conjugated antibodies (7-Aminoactinomycin D (7-AAD, BD), GR-1 (BioLegend), B220 (BioLegend), and TER-119 (BioLegend)). Cells were then sorted using a FACS ARIA II (BD) by eliminating dead cells (7AAD-), myeloid-derived suppressor cells (MDSCs; GR-1-), B-cells (B220-), and erythroid cells (TER-119-). The sorted PD-1$^{KO}$ and WT T-cells were mixed at a 1:1 ratio and intravenously (i.v.) adoptively transferred (5 x 103 cells) to C57BL/6J CD45.2$^{+}$ mice bearing day 5 B16-OVA tumors.

To control for potential effects of the different congenic markers expressed by the PD-1$^{KO}$ and WT T-cells (and confirm that neither marker alone has a competitive advantage), this process was repeated with two populations of naïve CD8$^{+}$ T-cells purified from different OT-I$^{+}$ WT mice, one expressing only CD45.1 (WT 1) and the

other expressing both CD45.1 and CD45.2 (WT 2) congenic markers. These two populations of WT T-cells were mixed at a 1:1 ratio and adoptively transferred to a separate group of day 5 tumor-bearing mice (as described above).

For Experiment 2, naïve OT-I$^{+}$ CD8$^{+}$ T-cells were isolated from the spleens of different OT-I$^{+}$ Cas9 mice, one expressing only CD45.2 and the other expressing both CD45.1 and CD45.2 congenic markers. The T-cells were transduced following the procedure described in Experiment 1, except that a lentiviral sgRNA expression vector with a Vex fluorescent reporter was added to the cells prior to the spin-infection at a multiplicity of infection (MOI) of 10. The CD45.1/CD45.2$^{+}$ T-cells were transduced with a *Pdcd1* sgRNA, creating a PD-1$^{KO}$ population. The CD45.2$^{+}$ T-cells were transduced with a non-targeting control sgRNA, creating a control population (CTL-1). The transduced OT-I$^{+}$ CD8$^{+}$ T-cells were sorted using a BD FACSARIA II (7-AAD$^{-}$, GR-1$^{-}$, CD45R$^{-}$, TER-119$^{-}$, Vex$^{+}$), then the PD-1$^{KO}$ and CTL-1 T-cells were mixed at a 1:1 ratio, and i.v. transferred to C57BL/6J CD45.2$^{+}$ mice bearing day 5 B16-OVA tumors. Due to low transduction efficiency, only 1 x $10^{3}$ T-cells were adoptively transferred compared to the 5 x $10^{3}$ transferred in Experiment 1.

A second control population (CTL-2) was also generated by transducing the Cas9 CD45.1/CD45.2$^{+}$ T-cells with a different non-targeting sgRNA (as described above). CTL-1 and CTL-2 T-cell populations were then mixed at a 1:1 ratio and adoptively transferred into a separate group of day 5 tumor-bearing mice. This was to ensure that the CTL-1 sgRNA used in the competitive assay with the *Pdcd1* sgRNA has no innate advantage or disadvantage.

## Transferred T-cell Recovery

Initial testing showed that by day 9 or 10 post adoptive transfer the tumors began to be rejected (data not shown), thus all mice were CO2 sacrificed and the tissue collected by day 8 post adoptive transfer for assessment of transferred T-cell recovery. In addition to the tumor, the dLN, iLN, and spleen were collected from each mouse.

Tumor infiltrating lymphocytes were isolated based on the protocol by Juneja et al. (2017). Tumors were mechanically separated using a gentleMACS dissociator (Miltenyi Biotec) and then digested for 30 min at 37°C with collagenase type I (400 U/ml, Worthington Biochemical). Post digestion, tumors were Ammonium-Chloride-Potassium (ACK; Lonza)-lysed for 90 sec and passed through 70 μm cell strainers (BD Falcon). Peripheral blood mononuclear cells, including the transferred $CD8^+$ T-cells, were then collected using a Percoll gradient (40% and 70%). To recover lymphocytes from the dLN, iLN, and spleen, each organ was disassociated, ACK-lysed for 90 sec to remove red blood cells, and then passed through 70 μm cell strainers and pressed with a plunger to obtain a single cell suspension. Recovered cells from the tumor, dLN, iLN, and spleen were resuspended in buffer (Dulbecco's phosphate-buffered saline (DPBS) without calcium or magnesium, 1% FBS (Sigma), 2 mM EDTA (Gibco)) and stained with anti-mouse fluorescently conjugated antibodies (BioLegend). Antibodies include: anti-CD11b (M1/70), anti-CD3 (17A2), anti-CD8b (YTS156.7.7), anti-CD45.2 (104), and anti-CD45.1 (A20).

Flow cytometry data were collected on the LSR II (BD) and the CytoFlex (Beckman Coulter). Data analyses were performed using FlowJo software (Tree Star).

## Statistics

All statistical analysis was performed with Prism software (GraphPad) with statistical significance determined by p-values $<0.05$. A Student's paired t-test was used when comparing two measures within the same group, an unpaired t-test was used when comparing two groups, and a mixed-design two-way ANOVA was used for comparison of two groups across multiple time points

Table 1: sgRNA Oligonucleotides.

| Gene Target | sgRNA |
|---|---|
| *Pdcd1* | GACACACGGCGCAATGACAG |
| *Ptpn2* | ATGTGCACAGTACTGGCCAA |
| CTL-1 | GCTTTCACGGAGGTTCGACG |
| CTL-2 | GCTTTCACGGAGGTTCGACG |

*Constructed sgRNA oligonucleotides based on the CRISPR algorithm provided by the Broad Institute.*

Table 2. Primers for PCR amplification and sequencing for TIDE analysis.

| Gene Target | TIDE Primers Forward 5' - 3’ | TIDE Primer Reverse 5' - 3' | TIDE Sequencing Primer |
|---|---|---|---|
| *Pdcd1* | GTACAGGCTCCT TCCTCACAGC | TCCATCCCTTAAA GGTAAATGGGCA TC | GTACAGGCTCCT TCCTCACAGC |
| *Ptpn2* | GCTGAAGCCAGC TTGATGTTC | CCCCCAAGAATT CTTAAGACCATC | GCTGAAGCCAGC TTGATGTTC |

*TIDE primers Forward and Reverse were used for PCR amplification. TIDE sequencing primers refer to the PCR primer used for sequencing and subsequent TIDE analysis.*

# Chapter III.

# Results

## Experiment 1

### Conventional PD-$1^{KO}$ $CD8^+$ T-cells have a competitive advantage in B16-OVA tumors

To validate the competitive T-cell adoptive transfer system, in Experiment 1 naive OT-$I^+$ transgenic $CD8^+$ T-cells were isolated from conventional OT-$I^+$ PD-$1^{KO}$ and OT-$I^+$ WT mice with different CD45 congenic markers and then adoptively transferred at equal proportion (Figure 1) into C57BL/6J WT $CD45.2^+$ mice with day 5 B16-OVA tumors. We observed no differences in tumor growth between the experimental (PD-$1^{KO}$ vs. WT-1) and control (WT-1 vs. WT-2) groups post-transfer ($F_{(5, 60)}$= 0.3461, p=0.8828, Figure 2). Gating strategy for analyzing recovered transferred $CD8^+$ T-cells can be found in Figure 3. No differences were found in the total number of transferred T-cells recovered from any organ between the experimental and control groups ($t_{(9)}$=0.9987, p=0.1960; Figure 4).

Representative plots of recovered transferred T-cells from the tumor, dLN, iLN, and spleen from both the experimental and control group are shown in Figure 5. In the experimental group, we found significantly greater enrichment of the PD-$1^{KO}$ T-cells within the tumors compared to the WT T-cells ($t_{(6)}$=7.551, p=0.0003; Figure 6). The PD-$1^{KO}$ T-cells were also found to have a competitive advantage over WT T-cells in the dLN ($t_{(5)}$=7.448, p=0.0007; Figure 6). In the control group, CD45 congenic marker expression appeared to have no effect on T-cell enrichment, as no significant differences were found

in the proportion of the transferred WT T-cells in the tumor ($t_{(5)}$=2.025, p=0.0988; Figure 6) or the draining lymph ($t_{(4)}$=2.418, p=0.0729; Figure 6). For both the experimental and control groups, too few of the transferred T-cells were recovered from the spleen or the iLN for any statistical comparisons to assess competitive advantages (Figure 4; Figure 5).

## Experiment 2

### CRISPR-Cas9 generated PD-1KO CD8+ T-cells have a competitive advantage in B16-OVA tumors

Given Experiment 1 showed that conventional OT-I$^{+}$ PD-1$^{KO}$ T-cells outcompeted OT-I$^{+}$ WT T-cells in the B16-OVA tumor microenvironment, in Experiment 2 we determined whether this outcome could be replicated with CRISPR-Cas9 mediated OT-I$^{+}$ PD-1$^{KO}$ T-cells. T-cells isolated from Cas9 mice were transduced with a lentiviral vector with Vex fluorescent reporter carrying either an sgRNA targeting *Pdcd1* (PD-1$^{KO}$), or one of two non-targeting control sgRNAs (CTL-1 or CTL-2); the transduced T-cells were then sorted based on Vex expression (Figure 7). For the experimental group, PD-1$^{KO}$ and CTL-1 T-cells were mixed at an equal proportion and adoptively transferred into C57BL/6 45.2$^{+}$ mice bearing day 5 B16-OVA tumors; this process was repeated for the control group, by mixing and adoptively transferring an equal proportion of CTL-1 and CTL-2 transduced T-cells (Figure 8). We observed no differences in tumor growth between the experimental and control group post-transfer ($F_{(4, 20)}$=0.9557 p=0.4530; Figure 9).

Gating strategy for analyzing recovered transferred CD8$^{+}$ T-cells can be found in Figure 10. No differences were found in the total number of transferred T-cells recovered

from any organ between the experimental group and control group ($t_{(6)}$=0.1948, p=0.2333; Figure 11). Representative plots of recovered transferred T-cells from tumor, dLN, iLN, and spleen from both the experimental and control group are shown in Figure 12. In the experimental group, we found significantly greater enrichment of the PD-$1^{KO}$ T-cells compared to the CTL-1 T-cells in the tumor ($t_{(3)}$=3.462, p=0.0406; Figure 13), confirming that the PD-$1^{KO}$ T-cells had a competitive advantage in the tumor microenvironment. In the control group, the non-targeting sgRNA appeared to have no effect on T-cell enrichment, as no significant differences were found in the proportion of the transferred CTL T-cells in the tumor ($t_{(3)}$=0.4364, p=0.692; Figure 13). For both the experimental and control groups, too few of the transferred T-cells were recovered from the lymph nodes or the spleen for any statistical comparisons to assess competitive advantages (Figure 11; Figure 12).

## Experiment 3

### CRISPR-Cas9 can edit multiple genes within the same genome

To expand on the single target CRISPR-Cas9 method used in Experiment 2, we wanted to establish in Experiment 3 that the CRISPR-Cas9 system could be used to perturb multiple genes within the same genome. We transduced B16-Cas9 tumor cells with two sgRNA vectors each creating 4 groups: 1) $Vex^+$ *Ptpn2* sgRNA and $Vex^+$ Control-1 sgRNA, 2) $RFP^+$ *Pdcd1* sgRNA and $RFP^+$ Control-2 sgRNA, 3) $RFP^+$ *Pdcd1* sgRNA and $Vex^+$ *Ptpn2*, and 4) $Vex^+$ Control-1 sgRNA and $RFP^+$ Control-2 sgRNA.

After incubation to allow for Cas9 editing, cells transduced with both sgRNA guides in each group were sorted based on Vex and RFP expression (Figure 14A). A TIDE assay was then performed using the isolated DNA from each group to determine if Cas9 was capable of editing both the *Pdcd1* and the *Ptpn2* genes within the same genome. Editing of both genes was successful, with an efficiency of approximately 42% for both *Pdcd1* and *Ptpn2* (Figure 14B).

## Experiment 4

### Cells transduced with Cre-ER$^{T2}$ express Cre intracellularly

While the constitutive CRISPR-Cas9 vector used in Experiments 2 and 3 allows for the editing of genes prior to adoptive T-cell transfers, we wanted to modify the vector in Experient 4 to allow for inducible editing of T-cells after adoptive transfer. The Vex-expressing constitutive CRISPR-Cas9 vector was modified into an inducible vector via the insertion of a loxP-stop-loxP within the tracrRNA sequence and the insertion of Cre-ER$^{T2}$ downstream of the tracrRNA. HEK-293x cells were transduced with the inducible vector in Experiment 4, and the vector was validated was based on Vex and Cre expression via flow cytometry (Figure 15).

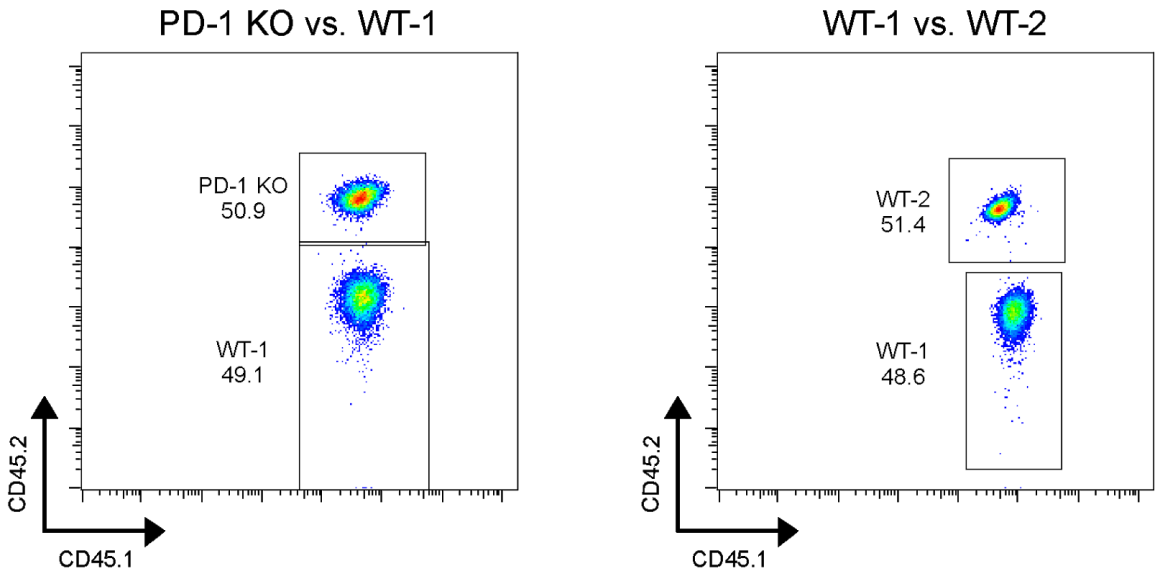


Figure 1. Input Ratios for Experiment 1

*Input ratios for the adoptive transfers of OT-I$^{+}$ CD8$^{+}$ T-cells into day 5 B16-OVA tumor-bearing mice based on CD45 markers. Outlined regions (gates) represent cells (dots) that were selected. The left plot represents the input ratio for the experimental group containing CD45.1/CD45.2 PD-1KO and CD45.1 WT T-cells. The right plot represents the input ratio for the control group containing CD45.1 WT-1 and CD45.1/CD45.2 WT-2 T-cells.*

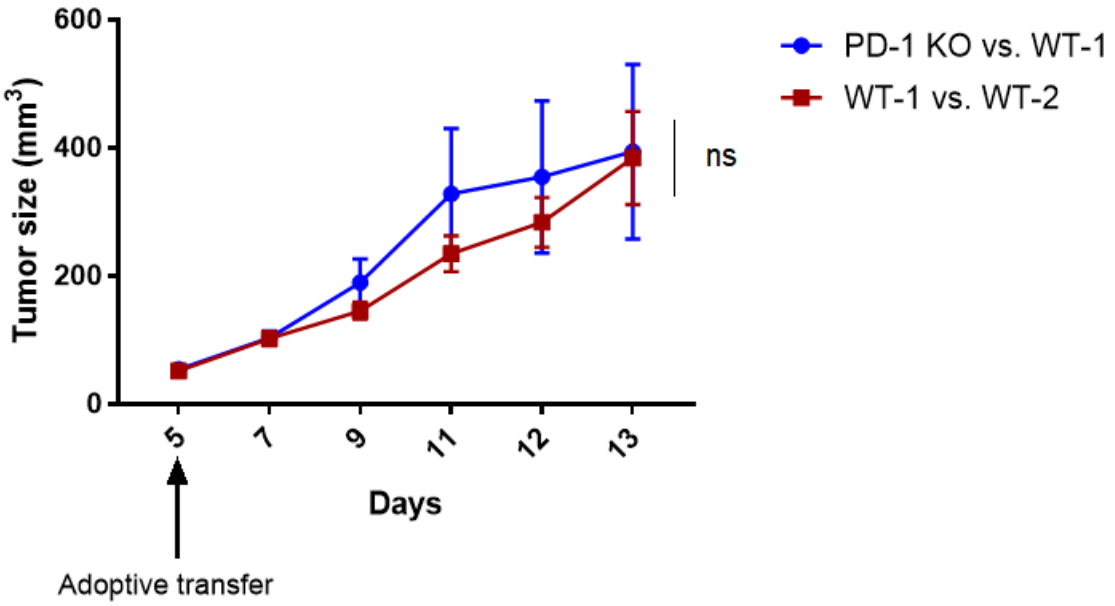


Figure 2. B16-OVA Tumor Growth Curves for Experiment 1

*C57BL/6J WT CD45.2$^{+}$ were injected s.c. in the right flank with 2 x 10$^{6}$ B16-OVA tumor cells. On day 5, OT-I$^{+}$ CD8$^{+}$ T-cells were i.v. transferred to the mice, at a 1:1 ratio of either PD-1$^{KO}$:WT-1 (n=7) or WT-1:WT-2 (n=7). Starting at 5 days after implantation, tumors were measured every 1-2 days and on the day of collection. Mice were euthanized and tissue collected on day 13. Statistical significance was determined by a two-way ANOVA. ns= not significant. Data shown as mean ± SEM.*

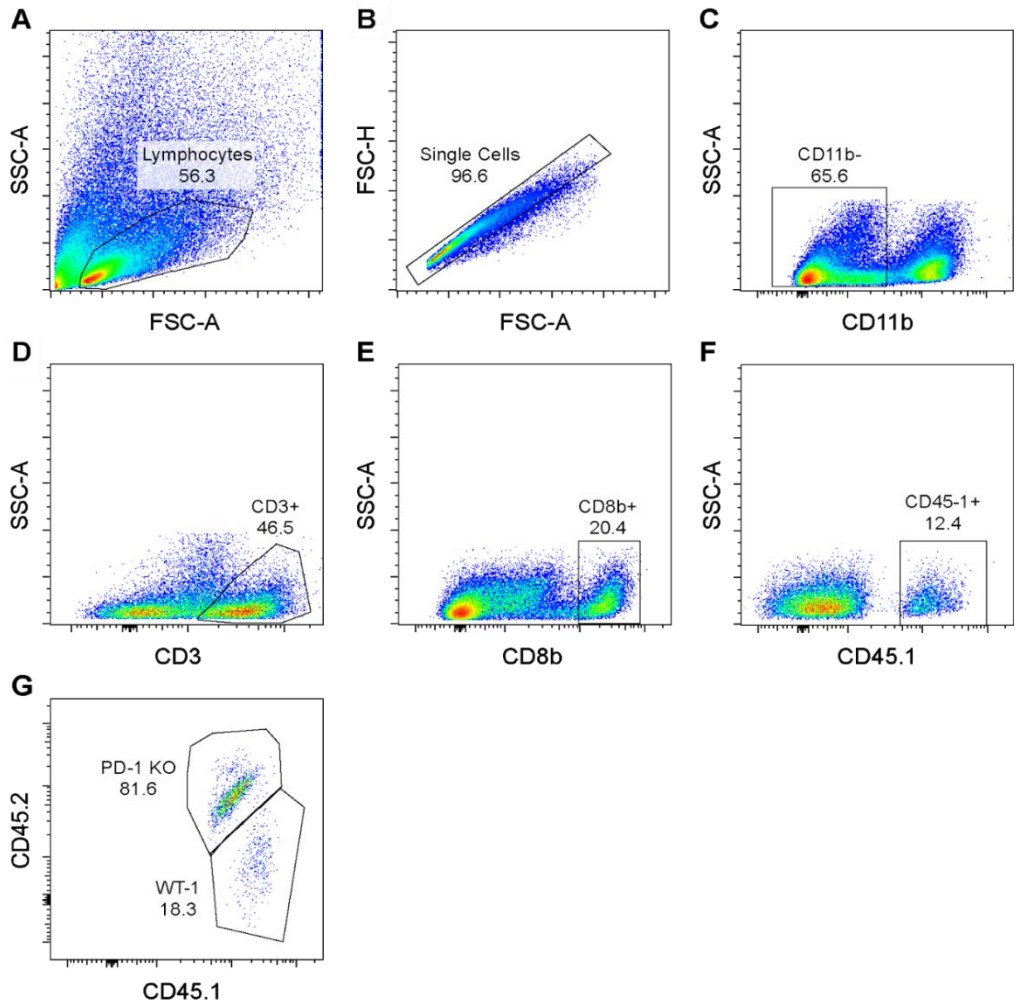


Figure 3. Gating Strategy for Experiment 1

*Flow cytometry analysis of T-cells isolated from tumor, spleen, and lymph nodes in Experiment 1 (depicted is the data for T-cells isolated from a tumor in the experimental group). Outlined regions (gates) represent cells (dots) that were selected. Plots B-G represent events within the previous plot's gate. (A) Side scatter area and forward scatter area plot displaying cell size to determine lymphocyte population. (B) Forward scatter area and height to select for single cells events and remove debris. (C) Gating to exclude cells expressing CD11b, which is a marker for innate immune cells. (D) Selecting for the T-cell marker, CD3. (E) Selecting for the CD8 marker, to exclude non-CD8$^{+}$ T-cells. (F) Selecting for the congenic marker CD45.1, which is expressed by all adoptively transferred cells. This excludes endogenous T-cells, which express only CD45.2. (G) Gating to determine recovered ratios of transferred PD-1$^{KO}$ and WT-1 T-cells, based on CD45.1 on the X axis and CD45.2 on the Y axis.*

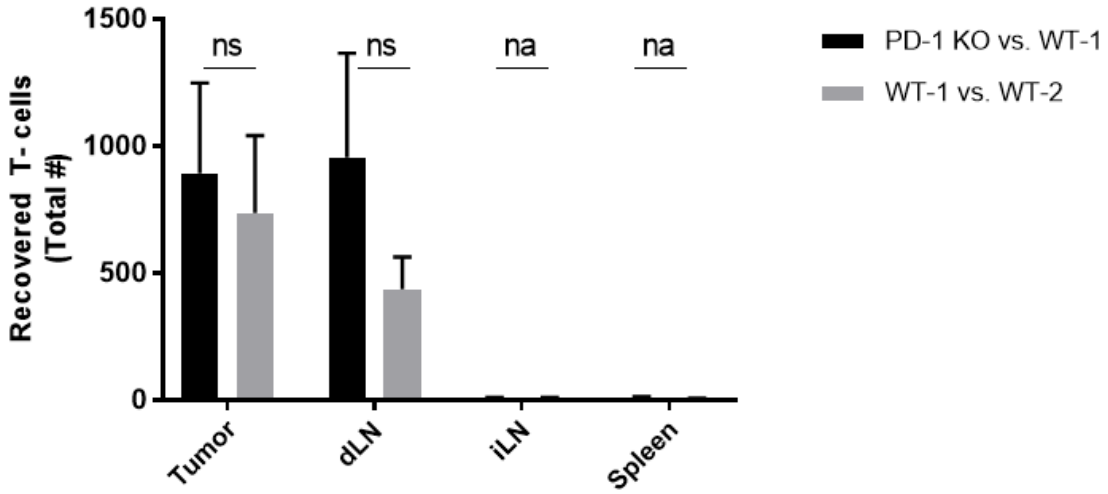


Figure 4. Recovery of Adoptively Transferred T-cells for Experiment 1

*Total OT-I$^{+}$ CD8$^{+}$ T-cell numbers based on the 45.1 expression of CD8$^{+}$ cells from tumor, draining lymph node (dLN), irrelevant lymph node (iLN), and spleen (data shown as mean ± SEM). Statistical significance was determined by Student's unpaired t-tests. ns = not significant, na = not analyzed.*

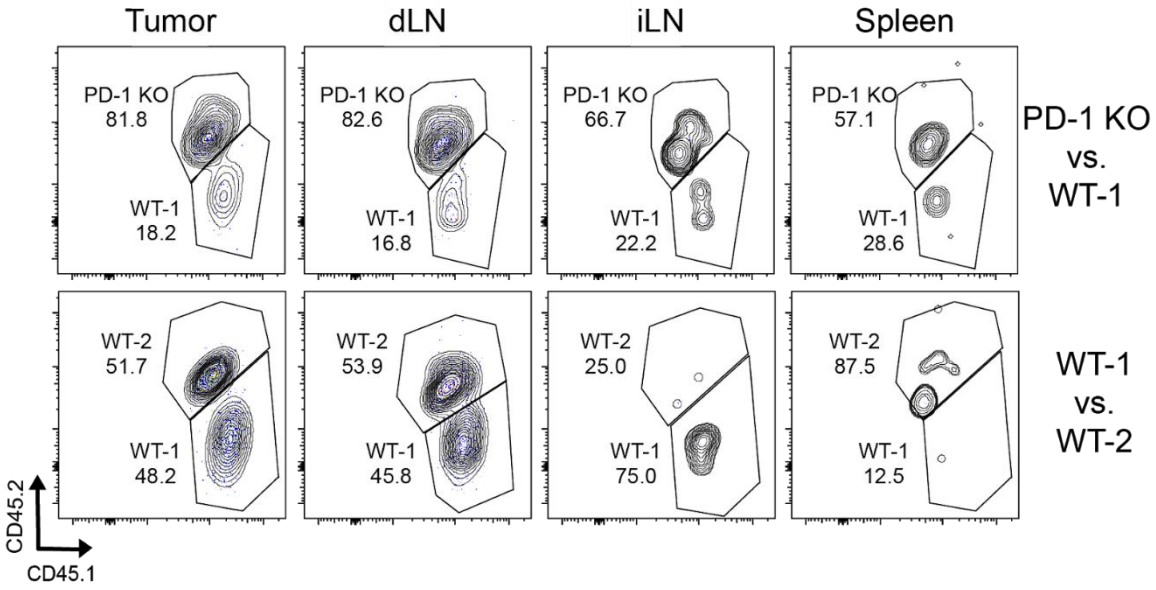


Figure 5. Representative Output Flow Cytometry Plots for Experiment 1

*OT-I$^{+}$ CD8$^{+}$ T-cells isolated from the tumor, draining lymph node (dLN), irrelevant lymph node (iLN), and spleen from mice in the experimental group (PD-1 $^{KO}$ vs. WT-1; top) and control group (WT-1 vs. WT-2; bottom). Outlined regions (gates) represent cells (dots) that were selected. Due to the low number of transferred T-cells recovered from the spleen and iLN, the dot plot was overlaid with a contour plot to better visualize the cell populations.*

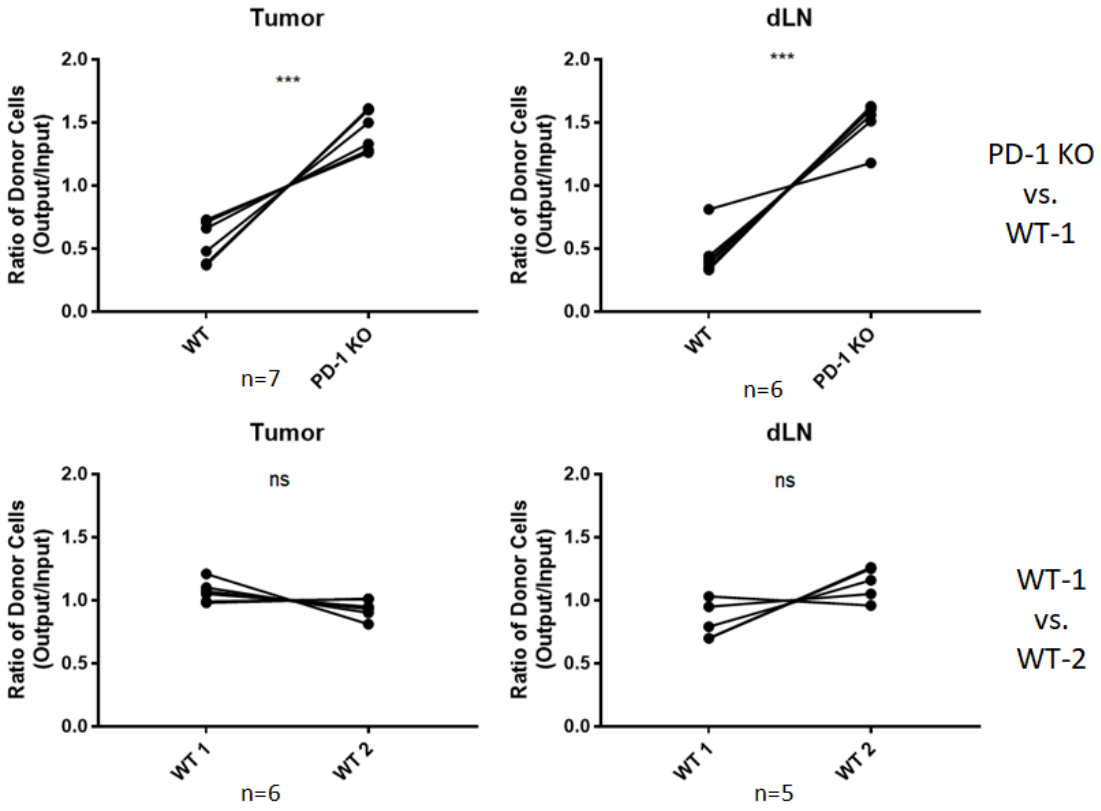


Figure 6. Output Ratio of Donor Cells for Experiment 1

*Ratio of collected OTI$^{+}$ CD8$^{+}$ T-cells (Figure 3) relative to the original input ratios (Figure 2) for the B16-OVA tumor (left) and draining lymph node (dLN; right) of mice in the experimental group (PD-1$^{KO}$ vs. WT-1; top) and control group (WT-1 vs. WT-2; bottom). Data for the following were not collected due to poor recovery of transferred T-cells: 1 dLN sample from the experimental group, 1 tumor sample and 2 dLN samples from the control group. Statistical significance was determined by Student's paired t-tests. ns = not significant, *** $p<0.001$.*

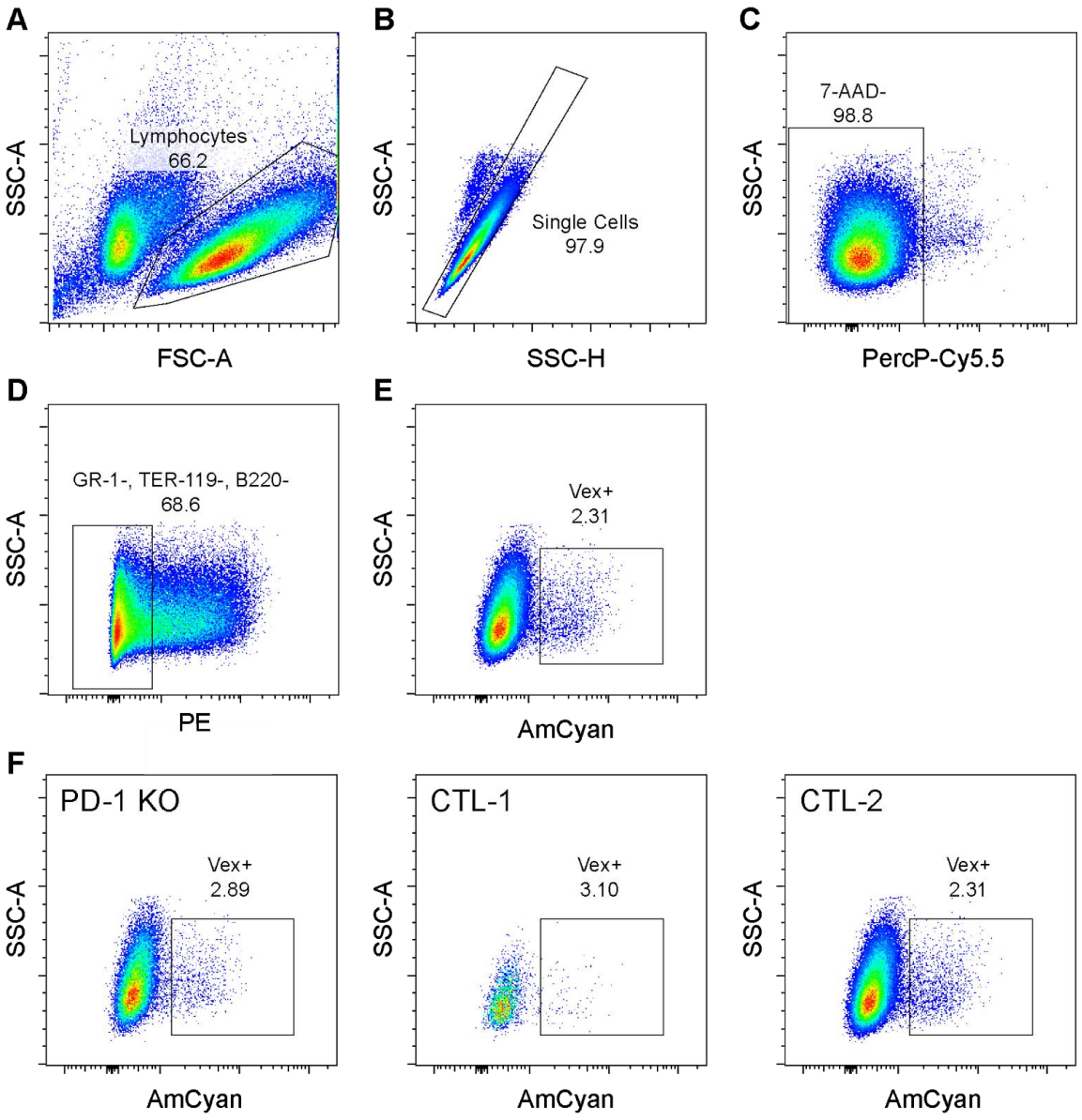


Figure 7. Sorting Strategy for Transduced Cas9 OT-I$^{+}$CD8$^{+}$T-cells in Experiment 2

*(A) Side scatter area and forward scatter area plot displaying cell size to determine lymphocyte population. (B) Forward scatter area and height to select for single cells events and remove debris. (C) Exclusion of dead cells via 7-AAD (D) Exclusion of B-cells, MDSCs, and erythroid cells. (E) Selecting for transduced, Vex$^{+}$ T-cells (F) Flow cytometry plots showing the percent of OT-I$^{+}$ CD8$^{+}$ T-cells transduced with the Pdcd1 sgRNA or with the non-targeting CTL-1 or CTL-2 sgRNAs.*

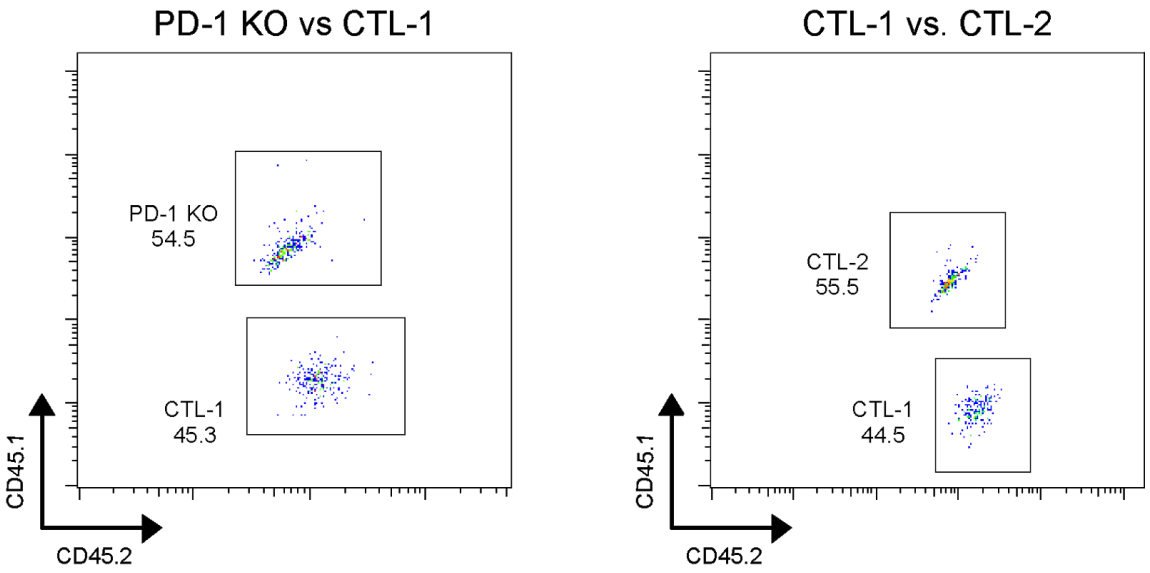


Figure 8. Input Ratios for Experiment 2

*Adoptive transfers input of OT-I$^{+}$ T-cells into day 5 B16-OVA tumor-bearing mice based on CD45 markers. Outlined regions (gates) represent cells (dots) that were selected. The left plot represents the input ratio for the experimental group containing CD45.1/CD45.2$^{+}$ T-cells transduced with a PD-1 targeting sgRNA and CD45.2$^{+}$ T-cells transduced with a non-targeting control sgRNA. The right plot represents the ratio for the control group containing CD45.1/CD45.2$^{+}$ and CD45.2$^{+}$ T-cells, each of which were transduced with a different non-targeting control sgRNAs.*

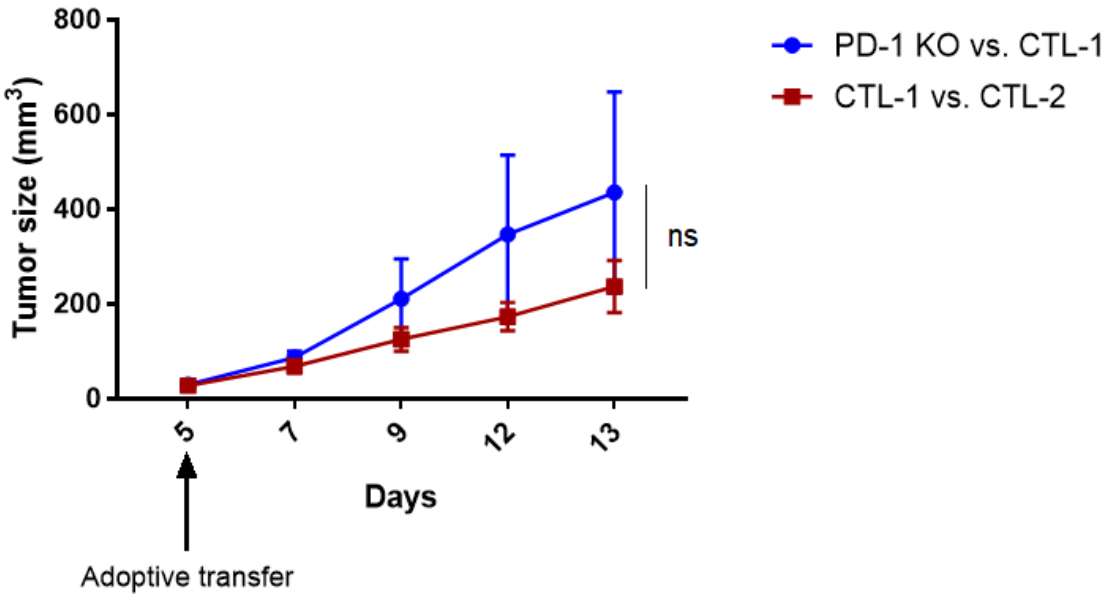


Figure 9. B16-OVA Tumor Growth Curves in Experiment 2

*C57BL/6J WT CD45.2$^{+}$ were injected s.c. in the right flank with 2 x 10$^{6}$ B16-OVA tumor cells. On day 5, sgRNA transduced OT-I$^{+}$ CD8$^{+}$ Cas9 T-cells were i.v. transferred to the mice, at a 1:1 ratio of either PD-1$^{KO}$:CTL-1 (n=4) or CTL-1:CTL-2 (n=4). Starting at 5 days after implantation, tumors were measured every 2-3 days and on the day of collection. Mice were euthanized and tissue collected on day 13. Mice were euthanized and tissue collected on day 13. Statistical significance was determined by a two-way ANOVA. ns= not significant. Data shown as mean ± SEM.*

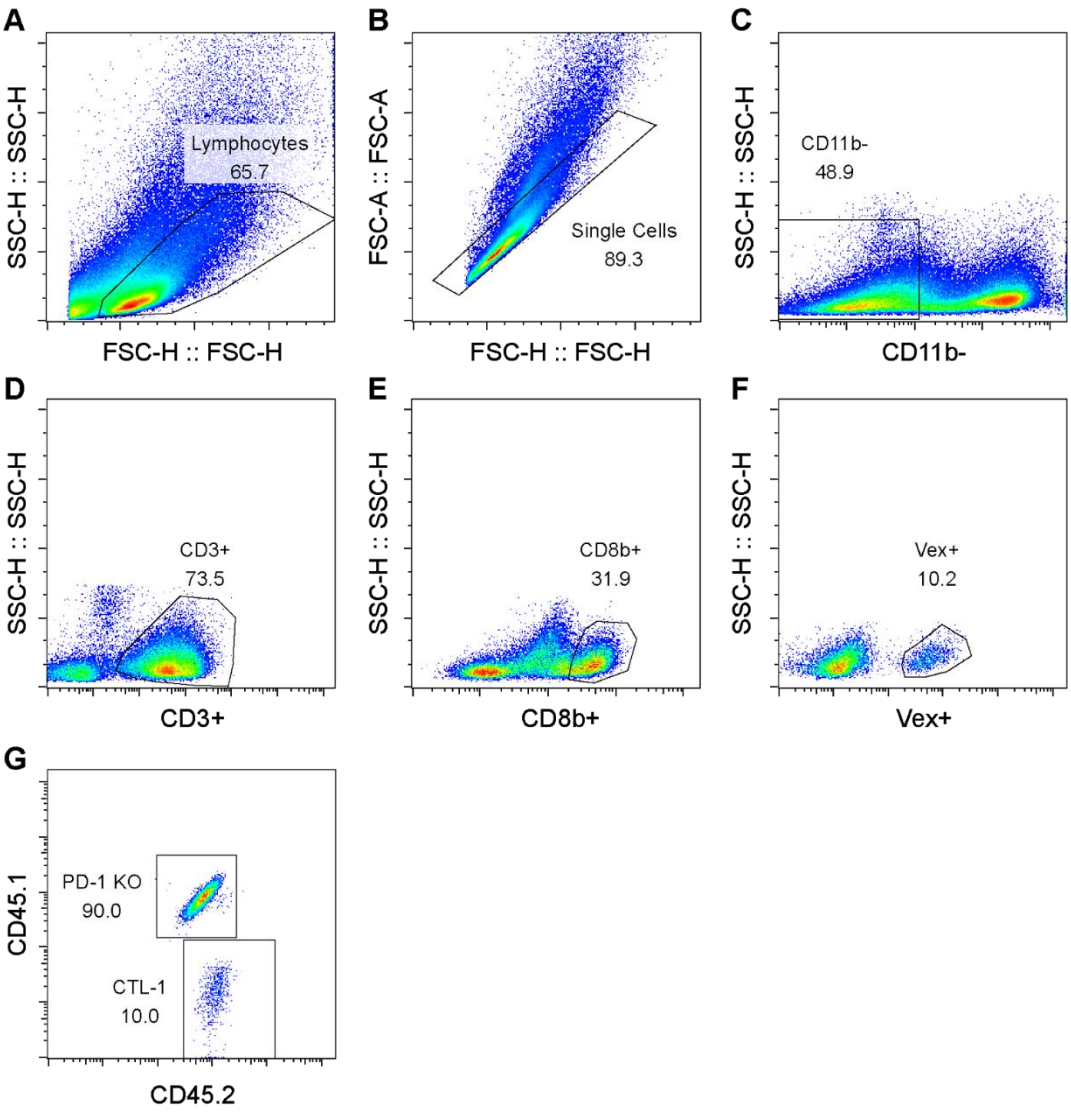


Figure 10. Gating Strategy for Experiment 2

*Flow cytometry analysis of T-cells isolated from tumor, spleen, and lymph nodes in Experiment 2 (depicted is the data for T-cells isolated from a tumor in the experimental group). Outlined regions (gates) represent cells (dots) that were selected. Plots B-F represent events within the previous plot's gate. (A) Side scatter area and forward scatter area plot displaying cell size to determine lymphocyte population. (B) Forward scatter area and height to select for single cells events and remove debris. (C) Gating to exclude cells expressing CD11b, which is a marker primarily for innate immune cells. (D) Selecting for the T-cell marker, CD3. (E) Selecting for the CD8 marker, to exclude non-$CD8^+$ T-cells. (F) Selecting for the Vex expression, which is expressed by all adoptively transferred cells, to excludes endogenous T-cells (G) Gating to determine recovered ratios of transferred PD-$1^{KO}$ and CTL-1 T-cells, based on CD45.2 on the X axis and CD45.1 on the Y axis.*

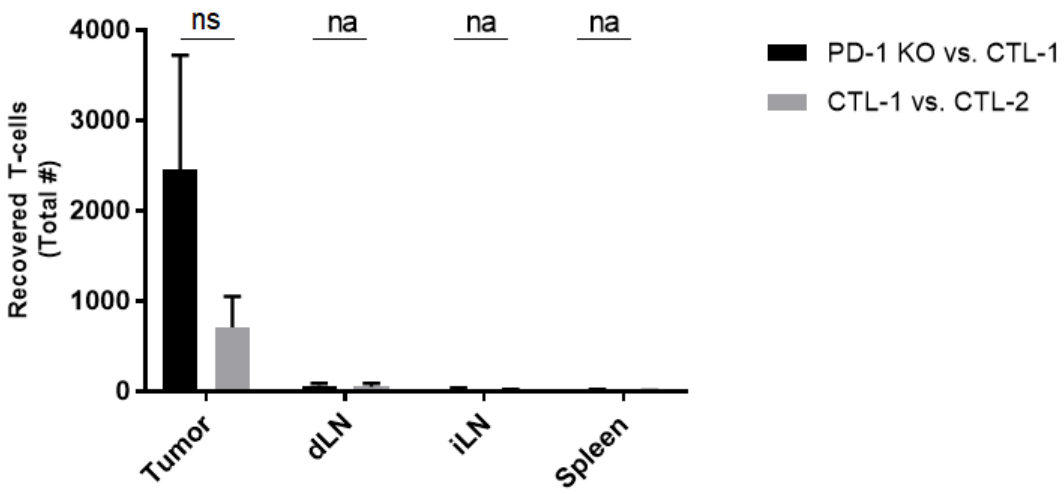


Figure 11. Recovery of Adoptively Transferred T-cells for Experiment 2

*Total Cas9 OT-I$^{+}$ CD8$^{+}$ T-cells from the B16-OVA tumor, draining lymph node (dLN), irrelevant lymph node (iLN), and spleen (data shown as mean ± SEM). Statistical significance was determined by Student's unpaired t-tests. ns = not significant, na = not analyzed.*

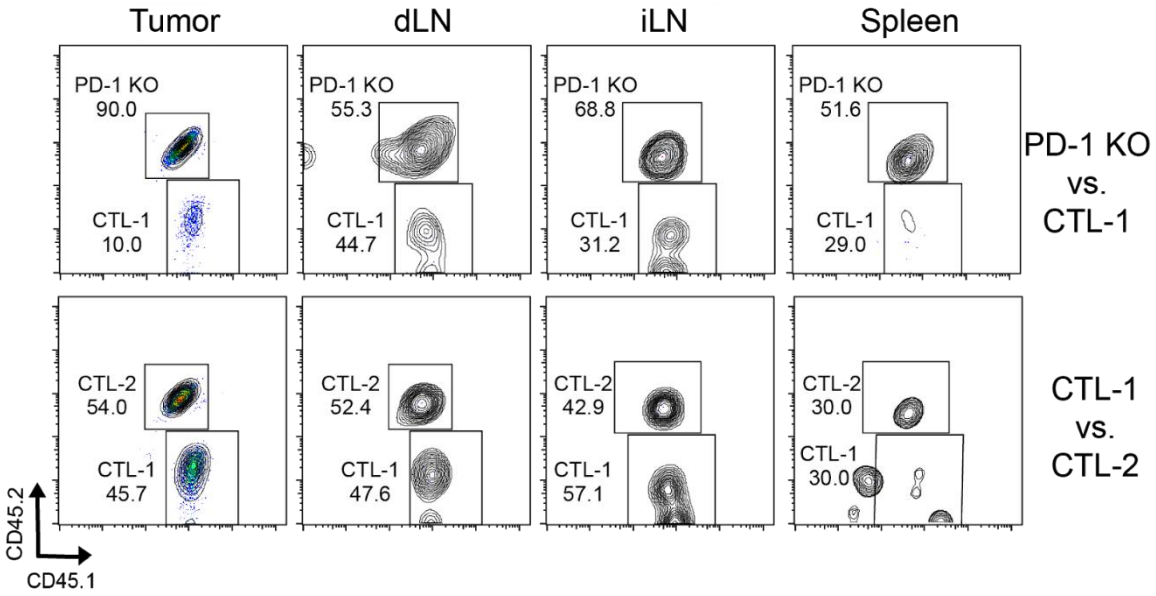


Figure 12. Representative Output Flow Cytometry Plots for Experiment 2

*Representative output flow cytometry plots of adoptively transferred Cas9 OT-I$^{+}$ CD8$^{+}$ T-cells recovered from B16-OVA tumor, draining lymph node (dLN), irrelevant lymph node (iLN), and spleen from mice in the experimental group (PD-1$^{KO}$ vs CTL-1; top) and control group (CTL-1 vs CTL-2; bottom). Outlined regions (gates) represent cells (dots) that were selected. Due to the low number of transferred T-cells recovered from the spleen and iLN, the dot plot was overlaid with a contour plot to better visualize the cell populations.*

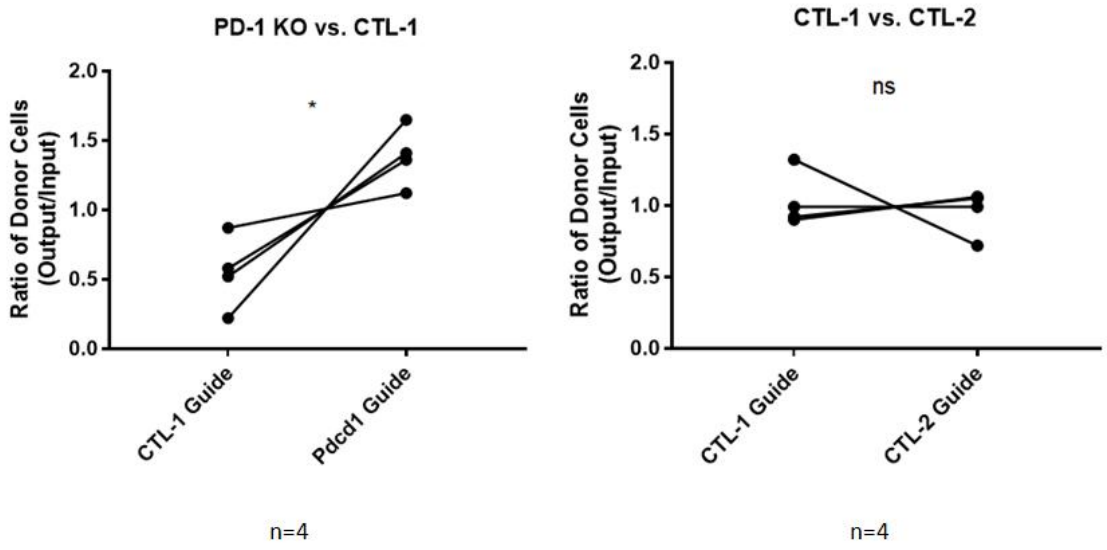


Figure 13. Output Ratio of Donor Cells in Experiment 2

*Ratio of collected Cas9 OT-I$^{+}$ CD8$^{+}$ T-cells (Figure 9) relative to the original input ratios (Figure 8) from the the B16-OVA tumor in the experimental group (PD-1$^{KO}$ vs. CTL-1; left) and control group (CTL-1 vs. CTL-2; right). Statistical significance was determined by Student's paired t-tests. ns = not significant, * $p<0.05$.*

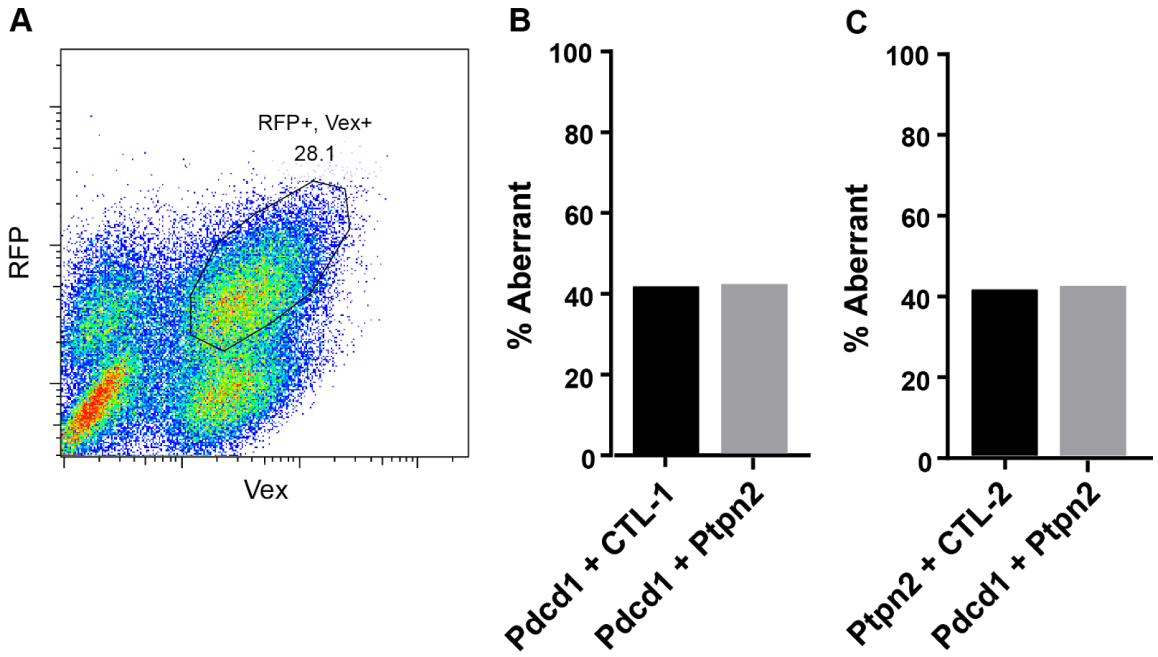


Figure 14. TIDE Assay for Experiment 3

*(A) Representative plot of sorting strategy to select for B16-Cas9 cells transduced with two sgRNAs simultaneously in Experiment 3. Outlined region (gate) represents cells (dots) sorted based on expression of both RFP and Vex. Cells that were positive for only RFP or Vex were excluded. TIDE assay on B16-Cas9 cells from (A) to determine the knockout percentage for Pdcd1 (B) or Ptpn2 (C) sgRNAs when combined with a non-targeting control sgRNA or each other. Knockout percentage is based on aberrant % sequence when compared to the non-targeting control sgRNAs (background aberrant sequence).*

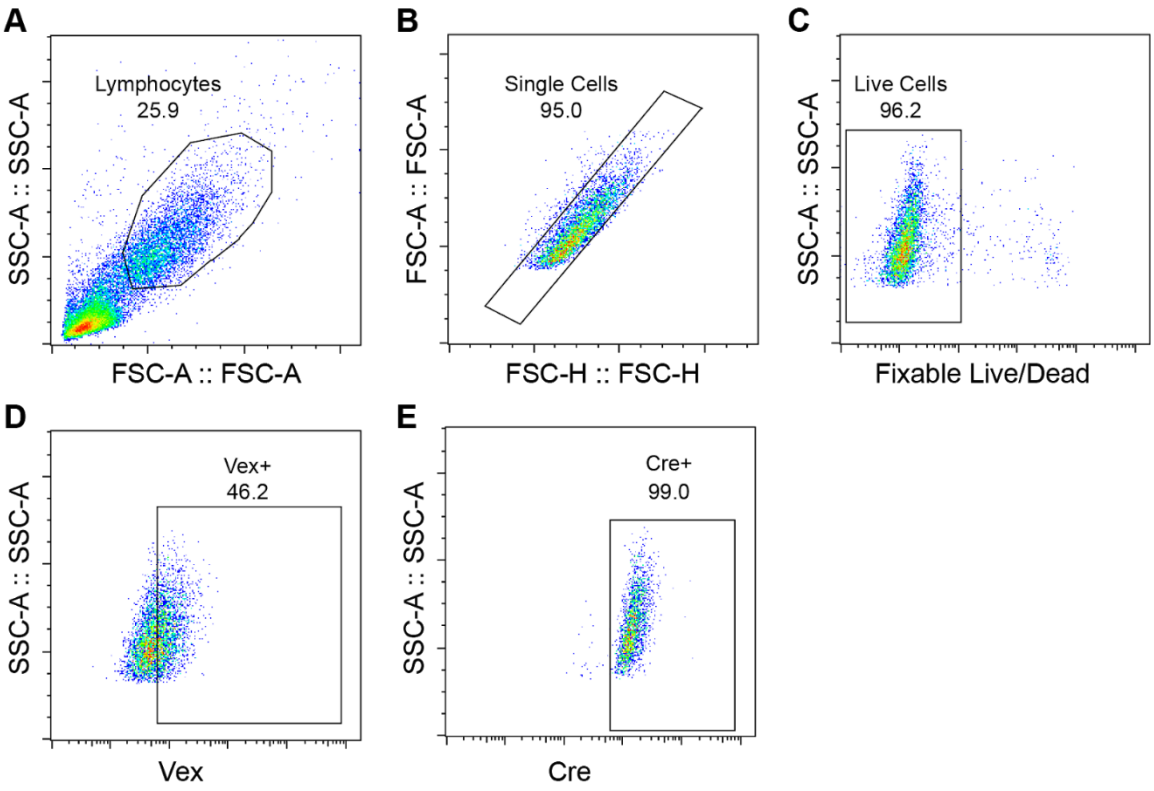


Figure 15: Gating Strategy and Cre Expression for Experiment 4

*Flow cytometry analysis of HEK-293X cells transduced with inducible CRISPR-Cas9 vector in Experiment 4. Outlined regions (gates) represents cells (dots) that were selected. Plots B-E represent events within the previous plot's gate. (A) Side scatter area and forward scatter area plot displaying cell size to determine HEK-293X population and remove debris. (B) Forward scatter area and height to select for single cells events and remove debris. (C) Exclusion of dead cells via fixable Live/Dead stain (D) Gating on transduced, $Vex^{+}$ cells (E) Gating on cytoplasmic Cre.*

# Chapter IV.

# Discussion

The primary goal of this thesis was to develop the tools necessary to create an *in vivo* based CRISPR-mediated knockout system that could be used to generate a genetic screen to discover novel negative regulators of T-cell dysfunction in the tumor microenvironment. Given the novelty of CRISPR editing technology, an *in vivo* based CRISPR-mediated T-cell screen had yet to be developed, thus in this thesis we conducted a series of experiments to validate the assays and techniques necessary to develop such a screening system. Here, we showed that we can determine T-cell advantages in the tumor microenvironment using a competitive adoptive T-cell transfer assay in tumor-bearing mice. Using this assay we found that conventional and CRISPR-mediated PD-$1^{KO}$ T-cells had a competitive advantage over WT T-cells in the tumor microenvironment, as indicated by a greater proportion of tumor-recovered T-cells being PD-$1^{KO}$ compared to WT. This confirmed that CRISPR-mediated PD-$1^{KO}$ T-cells perform similarly to conventional PD-$1^{KO}$ T-cells in the tumor microenvironment. We then successfully demonstrated that the CRISPR-Cas9 system is capable of editing two genes simultaneously within the same genome, an important step in the development of a screening system that will be capable of investigating gene interactions. Finally, we created an inducible CRISPR vector by inserting the Cre-$ER^{T2}$/loxP system into our constitutive CRISPR vector, which will allow for inducible genetic screens on T-cells after being adoptively transferred into tumor-bearing mice. Together, these experiments have made substantial progress toward our goal of the tools necessary to create

developing an *in vivo* based CRISPR-mediated screen to discover novel negative regulators of T-cell dysfunction in the context of tumors.

The ease of engineering and the affordability of modifying the sgRNA sequences make the CRISPR-Cas9 system an ideal method for performing large-scale genetic screens. Other knockout screens, like those using ZFN or TALENs, require researchers to painstakingly engineer a different protein for each new target, which is much more time consuming and cost-prohibitive than the generation of new sgRNAs (Boettcher & McManus, 2015). Additionally, genetic screens using RNAi are limited due to off-target effects and the incomplete suppression of the target genes (Boutros & Ahringer, 2008), while by comparison CRISPR-Cas9 results in complete gene knockout. In support of using CRISPR-Cas9, one study performed a CRISPR-Cas9 screen and an RNAi screen in parallel to identify essential genes in the human chronic myelogenous leukemia cell line K562 (Morgens, Deans, Li, & Bassik, 2016). They found that the CRISPR-Cas9 overall performed better, and identified more essential genes than the RNAi screen. However, results also showed surprisingly little correlation, and combining the two screens resulted in the best performance. For these reasons, we predict that genetic screens using CRISPR-editing technology will become the standard, though it is unlikely that they will completely replace other technologies.

## Conventional PD-1$^{KO}$ T-cells have a competitive advantage over WT T-cells in an *in vivo* adoptive transfer assay

In Experiment 1, we found that PD-1$^{KO}$ T-cells had a competitive advantage within the tumor microenvironment compared to WT T-cells (Figure 6), as expected based on previous work (Iwai, Terawaki, & Honjo, 2005). We hypothesized we would observe a similar effect in the dLN, but not in the iLN or the spleen. Due to the close proximity of the dLN to the tumor, the dLN acts as the primary location for T-cell priming and activation. However, the immunosuppressive effects of PD-L1 expression by the B16 tumors (Kleffel et al., 2015; Gupta et al., 2016) inhibits CD8$^{+}$ T-cell activation and function in the nearby dLN (Fransen, Arens, & Melief, 2013). Thus, PD-1 deficiency should provide resistance to the PD-L1 activity. The iLN and the spleen are immunological sites more separated from the effects B16 tumors compared to the dLN, thus should experience reduced priming and less immunosuppression. Confirming our hypothesis, we found that PD-1$^{KO}$ T-cells had a competitive advantage in the dLN (Figure 6), however too few transferred CD8$^{+}$ T-cells were recovered from the iLN or spleen for a statistical comparison (Figure 4; Figure 5).

It is unlikely that allowing the T-cells to compete *in vivo* for longer would result in greater enrichment of the transferred T-cells in the iLN or spleen. A previous study recovered considerably more transferred T-cells from the iLN and spleen despite collecting the transferred T-cells 7 days post-transfer cells, which was 1 day earlier than in our study (Zhou et al., 2014). This increased recovery compared to the current study may have resulted from methodological differences. Specifically, Zhou et al. implanted

fewer B16-OVA cells than the current study but allowed for 14 days of tumor growth prior to adoptive T-cell transfers (opposed to 5 days of growth in the current study). This extra growth time could have allowed for more B16 cells to separate from the tumor and circulate through the blood into the iLN and spleen, allowing for a greater likelihood of T-cell priming and activation and thus greater recovery of T-cells from these locations.

Since we used different CD45 congenic markers to distinguish the PD-$1^{KO}$ T-cells from the WT cells, we wanted to confirm that neither congenic marker conferred a competitive advantage within the tumor microenvironment. Thus we isolated $CD8^+$ T-cells from OT-$I^+$ CD45.$1^+$ mice and from OT-$I^+$ CD45.1/CD.$2^+$ mice and then adoptively transferred them at equal proportion into B16-OVA tumor-bearing mice (Figure 1). Our results showed no significant difference in the proportion of either WT population in either the tumor or the dLN, confirming that the competitive advantage of PD-$1^{KO}$ T-cells is due to the PD-1 deficiency, and not due to the CD45.1/CD45.2 congenic markers. These data show that the CD45 congenic markers can be used in future adoptive transfer T-cell screens without impacting T-cell competitiveness. Combined with the data from the experimental group, these results confirm that competitive adoptive transfer assays are an effective tool to assess T-cell advantages within the tumor microenvironment.

### CRISPR-mediated PD-$1^{KO}$ T-cells have a competitive advantage over WT T-cells in an *in vivo* adoptive transfer assay.

With the utility of the adoptive transfer system established in Experiment 1, we then aimed to use this system with CRISPR-edited $CD8^+$ T-cells. Thus in Experiment 2, we chose to repeat the adoptive T-cell transfer assay with CRISPR-mediated deletion of the PD-1 gene, *Pdcd1*, to see if it recapitulated the competitive advantage of conventional

PD-1$^{KO}$ CD8$^{+}$ T-cells in the context of B16 tumors we observed in Experiment 1. Based on the literature (Legut, Dolton, Mian, Ottmann, & Sewell, 2017), we hypothesized that the CRISPR-mediated knockouts should perform functionally the same as conventional knockouts.

To create CRISPR-mediated PD-1$^{KO}$ T-cells, we isolated naive CD8$^{+}$ T-cells from OT-I$^{+}$ Cas9 mice and then transduced the T-cells with a lentiviral vector with a Vex fluorescent reporter that carried either an sgRNA targeting *Pdcd1*, or a non-targeting control sgRNA. Based on the literature (Zhou et al., 2014; Ghassemi et al., 2016), we knew that T-cell transduction could be challenging, and required cytokine stimulation. Although we followed a protocol shown to be successful for transducing naive CD8$^{+}$ T-cells (Zhou et al., 2014), we had a very low transduction efficiency (Figure 7). Thus, the number of T-cells we adoptively transferred to each mouse in Experiment 2 was five times fewer than the number transferred in Experiment 1 ($1 \times 10^3$ vs. $5 \times 10^3$). In preliminary experiments we found that competitive adoptive T-cell transfers between $5 \times 10^3$ and $1 \times 10^4$ resulted in the best enrichment of the T-cells in the tumor and secondary lymphoid organs, however $1 \times 10^3$ was still sufficient for competition to occur.

Despite these limitations, we found greater enrichment CRISPR-mediated PD-1$^{KO}$ T-cells relative to the those transduced with a non-targeting control sgRNA in the tumor (Figure 13), replicating the main finding with conventional PD-1$^{KO}$ T-cells in Experiment 1. This confirmed our hypothesis that CRISPR-mediated PD-1$^{KO}$ T-cells perform functionally similar to conventional PD-1$^{KO}$ T-cells. However, unlike Experiment 1, we were unable to recover enough of the transferred T-cells from the dLN for statistical comparisons. We suspect that this is due to the low number of T-cells adoptively

transferred into the tumor-bearing mice. It is likely upon repeating with a larger pool of T-cells in our adoptive transfer, we would see improved T-cell recovery in the dLN, with similar enrichment of the PD-$1^{KO}$ T-cells relative control T-cells as seen in Experiment 1.

Since it is possible that the chosen non-targeting control guide had off-target effects, we wanted to compare it with another non-targeting control guide to confirm it had no functional impact on the T-cells. Thus we isolated $CD8^+$ T-cells from OT-$I^+$ Cas9 mice with different CD45 congenic markers and transduced each with a different non-targeting control sgRNA. We then adoptively transferred them at equal proportion into B16-OVA tumor-bearing mice (Figure 8). Our results showed no significant difference in the proportion of the control T-cell populations in the tumor, confirming that the competitive advantage of CRISPR-generated PD-$1^{KO}$ T-cells is due to the PD-1 deficiency. These data show that these non-targeting sgRNAs can be used in future adoptive transfer T-cell screens without impacting T-cell competitiveness.

These data demonstrate that the CRISPR-mediated genetic knockouts perform functionally similar to conventional knockout methods within the tumor microenvironment in competitive adoptive T-cell transfer assays. We can expand this system by performing CRISPR-mediated genetic screens on T-cells and then adoptively transferring them into the B16 tumor-bearing mice. This will provide a method a to discover novel regulators of T-cell dysfunction within the tumor microenvironment, based competitive T-cell advantages

## Transfer of PD-1$^{KO}$ T-cells had no effect on B16 tumor growth.

Despite the significant competitive advantage of PD-1$^{KO}$ T-cells to WT T-cells within the B16 tumor microenvironment, our data showed that adoptive transfers of PD-1$^{KO}$ T-cells had no effect on B16 tumor growth in either Experiment 1 or Experiment 2 (Figure 2; Figure 9). Previous studies have shown that PD-1 blockade significantly improves T-cell recruitment within the B16 tumors, but PD-1 treatment alone is ineffective at treating B16 tumors (Iwai, Terawaki, & Honjo, 2005; Chen et al., 2015; Kleffel et al., 2015). Thus, we would only expect to see differences in tumor growth between the treatment and control group PD-1 treatment was combined with another therapy, such as vaccination (Juneja et al., 2017).

However, given our observation of tumor rejection 8 days post adoptive transfer in both control and experimental groups, it appears that the binding specificity and affinity of the OT-I TCR expressed by the transferred CD8$^{+}$ T-cells was enough overcome the B16-OVA tumor immunosuppression, irrespective of PD-1 expression. Since the PD-1$^{KO}$ T-cells were more enriched in the tumors relative to the WT T-cells, we would expect to see a faster clearance of tumors in the experimental groups. It is likely that the tumors were collected before differences could be seen, however a later collection day would cause a reduction in the number of recovered transferred T-cells.

## The CRISPR-Cas9 system can simultaneously knockout two genes within the same genome

Most tumors require a combination of treatments for effective responses (Pardoll & Drake, 2012; Swart, Verbrugge, & Beltman, 2016). As a result, animal studies and

clinical trials have begun to shift focus towards combination therapies for the treatment of cancer, particularly combinations that include PD-1 checkpoint blockade (Curran, Montalvo, Yagita, & Allison, 2010; Robert et al., 2014; LaFleur, Muroyama, Drake, & Sharpe, 2018). A CRISPR-Cas9 combinatorial screen that perturbs multiple genes simultaneously could lead to the discovery to synergistic therapeutic effects in the context of tumors. Therefore, in addition to CRISPR-mediated single target loss-of-function screens, we wanted to establish that the CRISPR-Cas9 system could be used to perturb multiple genes within the same genome

As a proof of concept, in Experiment 3 we used a CRISPR-Cas9 vector and two sgRNAs to knockout both *Pdcd1* and *Ptpn2* within the same genome (Figure 14). Previous research has found that *Ptpn2* attenuates TCR signaling, and that *Ptpn2*-deficient $CD8^+$ T-cells have a lower threshold for TCR-instigated responses *in vivo*, which allows for a better response to antigen peptides with suboptimal TCR affinity (Wiede, Gruta, & Tiganis, 2014). Given that tumors often express weakly immunogenic antigens (Shankaran et al., 2001), our laboratory has recently shown that CRISPR-mediated $Ptpn2^{KO}$ T-cells have a competitive advantage in the MC38 colorectal tumor model (LaFleur et al., 2018). Therefore *Ptpn2* is an ideal candidate to test novel combination therapies, like PD-1 deficiency, for improving $CD8^+$ T-cell response in the tumor microenvironment.

In the current study, we simultaneously knocked out *Pdcd1* and *Ptpn2* in B16-Cas9 tumor cells, and thus showed that the CRISPR-mediated genetic knockout of multiple genes is possible. If we can replicate this double knockout in T-cells, we can then perform CRISPR-mediated screens on T-cells and adoptively them into the B16

tumor-bearing mice. This will provide a method to discover novel combination therapies that synergistically prevent or reverse T-cell dysfunction within the tumor microenvironment.

## The CreER$^{T2}$-lox system can create an inducible CRISPR-Cas9 system

The constitutive CRISPR vector utilized in Experiments 2 and 3 is useful for performing screens on CD8$^{+}$ T-cells to discover novel targets that prevent T-cell dysfunction when exposed to the immunosuppressive tumor microenvironment. However, it is also important to find novel therapeutic targets that are capable of reversing T-cell dysfunction in the tumor microenvironment. This is especially relevant for antibody checkpoint blockade therapies, where treatment success depends on reinvigoration of dysfunctional T-cells (Sakuishi et al., 2010; Zarour, 2016; Huang et al., 2017). The use of an inducible *in vivo* CRISPR-mediated screen has the potential for the discovery of novel targets that primarily reverse T-cell dysfunction, rather than just preventing dysfunction.

In Experiment 4, we disrupted transcription of the tracrRNA of the CRISPR-Cas9 vector by inserting a transcription terminator sequence flanked by loxP sites within the tracrRNA sequence. We also inserted a tamoxifen-dependent Cre-ER$^{T2}$ (Ruzankina et al., 2007) downstream of the tracrRNA sequence in the vector, thus transforming the constitutively expressing CRISPR-Cas9 vector used in Experiments 2 and 3 into an inducible vector. We confirmed the transduction of the inducible vector in HEK-293x cells based a fluorescent reporter, and the production the Cre protein (Figure 15).

In future experiments, we plan to test if this vector can be used for CRISPR-Cas9 editing of $CD8^+$ T-cells with various sgRNAs. If successful, we will then expand our competitive T-cell adoptive transfer system to perform an inducible CRISPR-mediated screen. Instead of editing the T-cells prior to an adoptive transfer into tumor-bearing mice, as done in Experiment 2, we could use the inducible system to edit T-cells post adoptive transfer by injecting the mice with 4-OHT, which allows for Cre catalytic activity by deactivating the fused estrogen-related receptor (Feil, Valtcheva, & Feil, 2009).

## Proposal for a CRISPR-mediated genetic screening system to discover novel negative regulators of T-cell dysfunction in the tumor microenvironment

Together, the experiments in this thesis have made substantial progress toward the goal of developing the tools necessary to create an *in vivo* based CRISPR-mediated genetic screening system able discover novel negative regulators of T-cell dysfunction in the tumor microenvironment. Such a screen will be useful to identify novel therapeutic targets for use in both checkpoint blockade and CAR T-cell therapies. Based on our data, we propose the following model for an *in vivo* based CRISPR-mediated T-cell genetic screening system. Specifically, we propose CRISPR-editing several populations of Cas9 $CD8^+$ T-cells with different sgRNAs and then adoptively transferring them into tumor-bearing mice. By then sequencing the recovered T-cells from the tumor and secondary lymphoid organs, competitive advantages can be determined based on over-representation of the an sgRNA relative to its input (Lafleur et al, 2018) similar to methods used in RNAi screens (Zhou et al., 2014). This method would be highly efficient

for conducting large-scale screens by allowing simultaneous assessment of the function of multiple gene targets. Once promising gene targets are identified in these large-scale screens, 1:1 competitive adoptive transfer assays like those used in Experiments 1 and 2 could be used to further validate the benefit of these individual gene targets on T-cell function.

We envision expanding this *in vivo* CRISPR-mediated system to include combinatorial screens that target multiple genes within the same genome of $CD8^+$ T-cells, using the double knockout technique developed in Experiment 3. Any discoveries from the single target screens could be used with each other, or with already established negative T-cell regulators (e.g., PD-1, CTLA-4, etc), in an *in vivo* based combination CRISPR-mediated screen using competitive adoptive transfer assays. Such combinatorial screens provide a method to discover the synergistic effects of targeting multiple targets simultaneously.

Lastly, we envision performing $CD8^+$ T-cell screens using the inducible CRISPR vector developed in Experiment 4, first in individual screens and later in combination screens using competitive adoptive transfer assays. This would allow for the discovery of therapeutic targets useful for reversing T-cell dysfunction within the tumor microenvironment, which has important implications for checkpoint blockade therapies.

## Research Limitations

As is the case with all animal models, discoveries and treatments that work with mouse models may not translate to humans. Therefore it is possible that any novel targets discovered as a result of the CRISPR-mediated screening system proposed in this thesis

may not translate to human clinical trials. However, antibodies used in checkpoint blockade in human clinical trials of cancer patients are based on checkpoints first discovered and tested in mouse models (Leach, Krummel, & Allison, 1996) so there is strong rationale for this approach.

While the adoptive transfer model proposed here has the potential to discover novel therapeutic targets, it is not without its limitations. In order to achieve meaningful frequencies of $CD8^+$ T-cell transduction using lentiviral vectors, stimulation and proliferation of the naïve T-cells is required. This is because efficient integration of the lentiviral vector into the T-cell genome requires T-cell activation via TCR and/or by cytokines (Verhoeyen, Costa, & Cosset, 2009). This stimulation, however, activates the $CD8^+$ T-cells before exposure to the OVA peptide so that it is no longer in a naïve state. This causes a reduction in T-cell priming and suboptimal activation when the $CD8^+$ TCRs do come into contact with OVA, resulting in reduced or atypical effector function. However, the stimulation of T-cells is also necessary for clinical trials using CAR T-cell therapy, and as such research using this method is still translatable to humans. For example, culturing T-cells with IL-7 and IL-15 as done in the current study, has been found to improve anti-tumor immunity of CAR T-cells in both the clinical setting (Xu et al., 2014) as well as in mouse models (Ghassemi et al., 2016).

Additionally, stimulation with IL-7 and IL-15 mitigates the effects of T-cell differentiation, as it causes the naive $CD8^+$ T-cells to develop into T memory stem ($T_{SCM}$) cells and sustain their expansion (Cieri et al., 2013). $T_{SCM}$ cells represent a rare subset of memory T-cells that are minimally differentiated and have phenotypic and functional characteristics similar to conventional naive T-cells (Ma, Koka, & Burkett, 2006;

Gattinoni, Speiser, Lichterfeld, & Bonini, 2017). Like naive T-cells, $T_{SCM}$ cells preferentially localize to the lymph nodes and are largely absent from mucosal surfaces (Lugli et al., 2013).

To avoid transducing the naïve T-cells directly one would have to transduce hematopoietic stem cells with the lentivirus vector, and then create bone marrow chimeric mice for each transduction (Godec et al., 2015). The process of creating a chimeric mouse and then using them for a competition assay requires a minimum of 8 weeks. Due to these limitations, bone marrow chimeras were beyond the scope of this thesis project. Additionally, the CRISPR-mediated genetic screening system method proposed here allows for a much higher throughput screen compared to bone marrow chimeras, thus increasing the potential discovery of immunotherapy targets. However, our laboratory has recently developed a chimeric CRISPR-Cas9 system to knockout of genes *in vivo* (LaFleur et al., 2018). Thus, in the future, it would possible to use the CRISPR-mediated genetic screening system method proposed in this thesis to test a wide-variety of genes, and follow-up any potential targets with more robust validation using the recently developed chimeric system.

Appendix 1.

Abbreviations

| | |
|---|---|
| 4-OHT | 4-hydroxytamoxifen |
| 7-AAD | 7-Aminoactinomycin D |
| ACK | Ammonium-Chloride-Potassium |
| APC | Antigen presenting cell |
| CAR | Chimeric antigen receptor |
| Cas9 | CRISPR associated protein 9 |
| CRISPR | Clustered regularly interspaced short palindromic repeats |
| CTL | Control |
| CTLA-4 | Cytotoxic T-lymphocyte -associated antigen 4 |
| dLN | Draining lymph node |
| DPBS | Dulbecco's phosphate-buffered saline |
| DMEM | Dulbecco's modified eagle medium |
| FBS | Fetal bovine serum |
| FDA | US Food and Drug Association |
| KO | Knockout |
| IL | Interleukin |
| iLN | Irrelevant lymph node |
| IFN-$\gamma$ | Interferon gamma |
| TNF-α | Tumor necrosis factor alpha |
| LAG-3 | Lymphocyte activation gene 3 protein |
| OT-I | Ovalbumin-specific TCR I |
| PD-1 | Programmed cell death protein 1 |
| PE | Phycoerythrin |
| *Ptpn2* | Tyrosine-protein phosphatase non-receptor type 2 |
| RFP | Red fluorescent protein |
| RNAi | RNA interference |
| RPMI | Roswell Park Memorial Institute medium |
| sgRNA | Single guide RNA |
| TALEN | Transcription activator-like effector nucleases |
| TCR | T-cell receptor |
| TIDE | Tracking of indels by decomposition |
| TIGIT | T-cell immunoreceptor with Ig and ITIM domains |
| TIL | Tumor infiltrating lymphocyte |
| TIM-3 | T-cell immunoglobulin domain and mucin domain protein 3 |
| TNF-α | Tumor necrosis factor alpha |
| $T_{SCM}$ | T memory stem cells |
| Vex | Violet-light-excited GFP |
| WT | Wild-type |
| ZNF | Zinc finger nuclease |

References

Allison, J. P. (1994). CD28-B7 interactions in T-cell activation. Current Opinion in Immunology, 6(3), 414–419. https://doi.org/10.1016/0952-7915(94)90120-1

Anderson M. T., Baumgarth N., Haugland R. P., Gerstein R. M., Tjioe T., Herzenberg L. A., & Herzenberg L. A. (1998). Pairs of violet-light-excited fluorochromes for flow cytometric analysis. Cytometry, 33(4), 435–444. https://doi.org/10.1002/(SICI)1097-0320(19981201)33:4<435::AID-CYTO7>3.0.CO;2-1

Anderson, A. C., Joller, N., & Kuchroo, V. K. (2016). Lag-3, Tim-3, and TIGIT co-inhibitory receptors with specialized functions in immune regulation. Immunity, 44(5), 989–1004. https://doi.org/10.1016/j.immuni.2016.05.001

Baumeister, S. H., Freeman, G. J., Dranoff, G., & Sharpe, A. H. (2016). Coinhibitory Pathways in Immunotherapy for Cancer. Annual Review of Immunology, 34(1), 539–573. https://doi.org/10.1146/annurev-immunol-032414-112049

Bhaijee, F., & Anders, R. A. (2016). PD-L1 Expression as a Predictive Biomarker: Is Absence of Proof the Same as Proof of Absence? JAMA Oncology, 2(1), 54–55. https://doi.org/10.1001/jamaoncol.2015.3782

Boettcher, M., & McManus, M. T. (2015). Choosing the Right Tool for the Job: RNAi, TALEN or CRISPR. Molecular Cell, 58(4), 575–585. https://doi.org/10.1016/j.molcel.2015.04.028

Boutros, M., & Ahringer, J. (2008). The art and design of genetic screens: RNA interference. Nature Reviews Genetics, 9(7), 554–566. https://doi.org/10.1038/nrg2364

Brinkman, E. K., Chen, T., Amendola, M., & van Steensel, B. (2014). Easy quantitative assessment of genome editing by sequence trace decomposition. Nucleic Acids Research, 42(22), e168. https://doi.org/10.1093/nar/gku936

Burnet, M. (1957). Cancer—A Biological Approach. British Medical Journal, 1(5023), 841–847.

Cameron, F., Whiteside, G., & Perry, C. (2011). Ipilimumab. Drugs, 71(8), 1093–1104. https://doi.org/10.2165/11594010-000000000-00000

Chen, L., & Flies, D. B. (2013). Molecular mechanisms of T-cell co-stimulation and co-inhibition. Nature Reviews. Immunology, 13(4), 227–242. http://doi.org/10.1038/nri3405

Chen, S., Lee, L.-F., Fisher, T. S., Jessen, B., Elliott, M., Evering, W., … Lin, J. C. (2015). Combination of 4-1BB Agonist and PD-1 Antagonist Promotes Antitumor Effector/Memory CD8 T Cells in a Poorly Immunogenic Tumor Model. Cancer Immunology Research, 3(2), 149–160. https://doi.org/10.1158/2326-6066.CIR-14-0118

Cieri, N., Camisa, B., Cocchiarella, F., Forcato, M., Oliveira, G., Provasi, E., … Bonini, C. (2013). IL-7 and IL-15 instruct the generation of human memory stem T cells from naive precursors. Blood, 121(4), 573–584. https://doi.org/10.1182/blood-2012-05-431718

Cong, L., Ran, F. A., Cox, D., Lin, S., Barretto, R., Habib, N., … Zhang, F. (2013). Multiplex Genome Engineering Using CRISPR/Cas Systems. Science (New York, N.Y.), 339(6121), 819–823. https://doi.org/10.1126/science.1231143

Curran, M. A., Montalvo, W., Yagita, H., & Allison, J. P. (2010). PD-1 and CTLA-4 combination blockade expands infiltrating T cells and reduces regulatory T and myeloid cells within B16 melanoma tumors. Proceedings of the National Academy of Sciences of the United States of America, 107(9), 4275–4280. https://doi.org/10.1073/pnas.0915174107

D'Aloia, M. M., Zizzari, I. G., Sacchetti, B., Pierelli, L., & Alimandi, M. (2018). CAR-T cells: the long and winding road to solid tumors. Cell Death & Disease, 9(3), 282. https://doi.org/10.1038/s41419-018-0278-6

Davila, M. L., Riviere, I., Wang, X., Bartido, S., Park, J., Curran, K., … Brentjens, R. (2014). Efficacy and Toxicity Management of 19-28z CAR T Cell Therapy in B Cell Acute Lymphoblastic Leukemia. Science Translational Medicine, 6(224), 224ra25-224ra25. https://doi.org/10.1126/scitranslmed.3008226

Doench, J. G., Fusi, N., Sullender, M., Hegde, M., Vaimberg, E. W., Donovan, K. F., … Root, D. E. (2016). Optimized sgRNA design to maximize activity and minimize off-target effects of CRISPR-Cas9. Nature Biotechnology, 34(2), 184–191. https://doi.org/10.1038/nbt.3437

Dunn, G. P., Bruce, A. T., Ikeda, H., Old, L. J., & Schreiber, R. D. (2002). Cancer immunoediting: from immunosurveillance to tumor escape. Nature Immunology, 3(11), 991–998. https://doi.org/10.1038/ni1102-991

Ehrlich, P. Ueber den jetzigen stand der Karzinomforschung. Ned. Tijdschr. Geneeskd. 5, 273–290 (1909).

FDA Approval for Ipilimumab. (2013). [WebContent]. Retrieved March 16, 2018, from https://www.cancer.gov/about-cancer/treatment/drugs/fda-ipilimumab

FDA approves CAR-T cell therapy to treat adults with certain types of large B-cell lymphoma (2017) [WebContent]. Retrieved March 15, 2018, from https://www.fda.gov/NewsEvents/Newsroom/PressAnnouncements/ucm581216.htm

Feil, S., Valtcheva, N., & Feil, R. (2009). Inducible Cre Mice. In Gene Knockout Protocols (pp. 343–363). Humana Press. https://doi.org/10.1007/978-1-59745-471-1_18

Fransen, M. F., Arens, R., & Melief, C. J. M. (2013). Local targets for immune therapy to cancer: Tumor draining lymph nodes and tumor microenvironment. International Journal of Cancer, 132(9), 1971–1976. https://doi.org/10.1002/ijc.27755

Gaj, T., Gersbach, C. A., & Barbas, C. F. (2013). ZFN, TALEN and CRISPR/Cas-based methods for genome engineering. Trends in Biotechnology, 31(7), 397–405. https://doi.org/10.1016/j.tibtech.2013.04.004

Gattinoni, L., Speiser, D. E., Lichterfeld, M., & Bonini, C. (2017). T memory stem cells in health and disease. Nature Medicine, 23(1), 18–27. https://doi.org/10.1038/nm.4241

Ghassemi, S., Bedoya, F., Nunez-Cruz, S., June, C., Melenhorst, J., & Milone, M. (2016). Shortened T cell culture with IL-7 and IL-15 provides the most potent chimeric antigen receptor (CAR)-modified T cells for adoptive immunotherapy. The Journal of Immunology, 196(1 Supplement), 214.23.

Germain, R. N. (2002). T-cell development and the CD4–CD8 lineage decision. Nature Reviews Immunology, 2(5), 309–322. https://doi.org/10.1038/nri798

Godec, J., Cowley, G. S., Barnitz, R. A., Alkan, O., Root, D. E., Sharpe, A. H., & Haining, W. N. (2015). Inducible RNAi *in vivo* reveals that the transcription factor BATF is required to initiate but not maintain $CD8^+$ T-cell effector differentiation. Proceedings of the National Academy of Sciences, 112(2), 512–517. https://doi.org/10.1073/pnas.1413291112

Gupta, H. B., Clark, C. A., Yuan, B., Sareddy, G., Pandeswara, S., Padron, A. S., … Curiel, T. J. (2016). Tumor cell-intrinsic PD-L1 promotes tumor-initiating cell generation and functions in melanoma and ovarian cancer. Signal Transduction and Targeted Therapy, 1, 16030. https://doi.org/10.1038/sigtrans.2016.30

Hammers, H. J., Plimack, E. R., Infante, J. R., Rini, B. I., McDermott, D. F., Lewis, L. D., … Amin, A. (2017). Safety and Efficacy of Nivolumab in Combination With Ipilimumab in Metastatic Renal Cell Carcinoma: The CheckMate 016 Study. Journal of Clinical Oncology: Official Journal of the American Society of Clinical Oncology, 35(34), 3851–3858. https://doi.org/10.1200/JCO.2016.72.1985

Hartmann, J., Schüßler-Lenz, M., Bondanza, A., & Buchholz, C. J. (2017). Clinical development of CAR T cells—challenges and opportunities in translating

innovative treatment concepts. EMBO Molecular Medicine, 9(9), 1183–1197. https://doi.org/10.15252/emmm.201607485

Hodi, F. S., O'Day, S. J., McDermott, D. F., Weber, R. W., Sosman, J. A., Haanen, J. B., … Urba, W. J. (2010). Improved survival with ipilimumab in patients with metastatic melanoma. The New England Journal of Medicine, 363(8), 711–723. https://doi.org/10.1056/NEJMoa1003466

Hogquist, K. A., Jameson, S. C., Heath, W. R., Howard, J. L., Bevan, M. J., & Carbone, F. R. (1994). T cell receptor antagonist peptides induce positive selection. Cell, 76(1), 17–27. https://doi.org/10.1016/0092-8674(94)90169-4

Hsu, P. D., Lander, E. S., & Zhang, F. (2014). Development and Applications of CRISPR-Cas9 for Genome Engineering. Cell, 157(6), 1262–1278. http://doi.org/10.1016/j.cell.2014.05.010

Hu, Z. (2017). The future of immune checkpoint blockade immunotherapy: towards personalized therapy or towards combination therapy. Journal of Thoracic Disease, 9(11), 4226–4229. https://doi.org/10.1016/j.cell.2014.05.010

Huang, A. C., Postow, M. A., Orlowski, R. J., Mick, R., Bengsch, B., Manne, S., … Wherry, E. J. (2017). T-cell invigoration to tumour burden ratio associated with anti-PD-1 response. Nature, 545(7652), 60–65. https://doi.org/10.1038/nature22079

Ikehara, S., Pahwa, R. N., Fernandes, G., Hansen, C. T., & Good, R. A. (1984). Functional T cells in athymic nude mice. Proceedings of the National Academy of Sciences, 81(3), 886–888. https://doi.org/10.1073/pnas.81.3.886

Iwai, Y., Terawaki, S., & Honjo, T. (2005). PD-1 blockade inhibits hematogenous spread of poorly immunogenic tumor cells by enhanced recruitment of effector T-cells. International Immunology, 17(2), 133–144. https://doi.org/10.1093/intimm/dxh194

Jiang, Y., Li, Y., & Zhu, B. (2015). T-cell exhaustion in the tumor microenvironment. Cell Death & Disease, 6(6), e1792. https://doi.org/10.1038/cddis.2015.162

Juneja, V. R., McGuire, K. A., Manguso, R. T., LaFleur, M. W., Collins, N., Haining, W. N., … Sharpe, A. H. (2017). PD-L1 on tumor cells is sufficient for immune evasion in immunogenic tumors and inhibits CD8 T cell cytotoxicity. Journal of Experimental Medicine, jem.20160801. https://doi.org/10.1084/jem.20160801

Keir, M. E., Freeman, G. J., & Sharpe, A. H. (2007). PD-1 Regulates Self-Reactive $CD8^+$ T Cell Responses to Antigen in Lymph Nodes and Tissues. The Journal of Immunology, 179(8), 5064–5070. https://doi.org/10.4049/jimmunol.179.8.5064

Kim, P. S., & Ahmed, R. (2010). Features of responding T cells in cancer and chronic infection. Current Opinion in Immunology, 22(2), 223–230. https://doi.org/10.1016/j.coi.2010.02.005

Kim, R., Emi, M., & Tanabe, K. (2007). Cancer immunoediting from immune surveillance to immune escape. Immunology, 121(1), 1–14. https://doi.org/10.1111/j.1365-2567.2007.02587.x

Kleffel, S., Posch, C., Barthel, S. R., Mueller, H., Schlapbach, C., Guenova, E., … Schatton, T. (2015). Melanoma cell-intrinsic PD-1 receptor functions promote tumor growth. Cell, 162(6), 1242–1256. https://doi.org/10.1016/j.cell.2015.08.052

Kvistborg, P., & Yewdell, J. W. (2018). Enhancing responses to cancer immunotherapy. Science, 359(6375), 516–517. https://doi.org/10.1126/science.aar6574

LaFleur, M. W., Muroyama, Y., Drake, C. G., & Sharpe, A. H. (2018). Inhibitors of the PD-1 Pathway in Tumor Therapy. Journal of Immunology (Baltimore, Md. : 1950), 200(2), 375–383. https://doi.org/10.4049/jimmunol.1701044

LaFleur, M.W.,Nguyen, T.H., Coxe, M.A., Trombley, J.D., Haining, N.W., Sharpe, A.H. (2018). Immunocut: A chimeric CRISPR-Cas9 system for knockout of genes*in vivo* in the hematopoietic system. Manuscript in preparation

Larkin, J., Hodi, F. S., & Wolchok, J. D. (2015). Combined Nivolumab and Ipilimumab or Monotherapy in Untreated Melanoma. The New England Journal of Medicine, 373(13), 1270–1271. https://doi.org/10.1056/NEJMc1509660

Leach, D. R., Krummel, M. F., & Allison, J. P. (1996). Enhancement of antitumor immunity by CTLA-4 blockade. Science (New York, N.Y.), 271(5256), 1734–1736.

Lee, D. W., Barrett, D. M., Mackall, C., Orentas, R., & Grupp, S. A. (2012). The Future Is Now: Chimeric Antigen Receptors as New Targeted Therapies for Childhood Cancer. Clinical Cancer Research : An Official Journal of the American Association for Cancer Research, 18(10), 2780–2790. http://doi.org/10.1158/1078-0432.CCR-11-1920

Legut, M., Dolton, G., Mian, A. A., Ottmann, O., & Sewell, A. (2017). CRISPR-mediated TCR replacement generates superior anticancer transgenic T-cells. Blood, blood-2017-05-787598. https://doi.org/10.1182/blood-2017-05-787598

Lugli, E., Dominguez, M. H., Gattinoni, L., Chattopadhyay, P. K., Bolton, D. L., Song, K., … Roederer, M. (2013). Superior T memory stem cell persistence supports long-lived T cell memory. The Journal of Clinical Investigation, 123(2), 594–599. https://doi.org/10.1172/JCI66327

Ma, A., Koka, R., & Burkett, P. (2006). Diverse functions of IL-2, IL-15, and IL-7 in lymphoid homeostasis. Annual Review of Immunology, 24, 657–679. https://doi.org/10.1146/annurev.immunol.24.021605.090727

Manguso, R. T., Pope, H. W., Zimmer, M. D., Brown, F. D., Yates, K. B., Miller, B. C., … Haining, W. N. (2017).*in vivo* CRISPR screening identifies *Ptpn2* as a cancer immunotherapy target. Nature, advance online publication. https://doi.org/10.1038/nature23270

Mani, R., St.Onge, R. P., Hartman, J. L., Giaever, G., & Roth, F. P. (2008). Defining genetic interaction. Proceedings of the National Academy of Sciences, 105(9), 3461–3466. https://doi.org/10.1073/pnas.0712255105

Morgens, D. W., Deans, R. M., Li, A., & Bassik, M. C. (2016). Systematic comparison of CRISPR/Cas9 and RNAi screens for essential genes. Nature Biotechnology, 34(6), 634–636. https://doi.org/10.1038/nbt.3567

Ngo, V. N., Davis, R. E., Lamy, L., Yu, X., Zhao, H., Lenz, G., … Staudt, L. M. (2006). A loss-of-function RNA interference screen for molecular targets in cancer. Nature, 441(7089), 106–110. https://doi.org/10.1038/nature04687

Pentcheva-Hoang, T., Egen, J. G., Wojnoonski, K., & Allison, J. P. (2004). B7-1 and B7-2 Selectively Recruit CTLA-4 and CD28 to the Immunological Synapse. Immunity, 21(3), 401–413. https://doi.org/10.1016/j.immuni.2004.06.017

Pardoll, D. M. (2012). The blockade of immune checkpoints in cancer immunotherapy. Nature Reviews. Cancer, 12(4), 252–264. https://doi.org/10.1038/nrc3239

Pardoll, D., & Drake, C. (2012). Immunotherapy earns its spot in the ranks of cancer therapy. The Journal of Experimental Medicine, 209(2), 201–209. https://doi.org/10.1084/jem.20112275

Postow, M. A., Chesney, J., Pavlick, A. C., Robert, C., Grossmann, K., McDermott, D., … Hodi, F. S. (2015). Nivolumab and Ipilimumab versus Ipilimumab in Untreated Melanoma. New England Journal of Medicine, 372(21), 2006–2017. https://doi.org/10.1056/NEJMoa1414428

Ribas, A., & Wolchok, J. D. (2018). Cancer immunotherapy using checkpoint blockade. Science, 359(6382), 1350–1355. https://doi.org/10.1126/science.aar4060

Robert, C., Ribas, A., Wolchok, J. D., Hodi, F. S., Hamid, O., Kefford, R., … Daud, A. (2014). Anti-programmed-death-receptor-1 treatment with pembrolizumab in ipilimumab-refractory advanced melanoma: a randomised dose-comparison cohort of a phase 1 trial. The Lancet, 384(9948), 1109–1117. https://doi.org/10.1016/S0140-6736(14)60958-2

Ruzankina, Y., Pinzon-Guzman, C., Asare, A., Ong, T., Pontano, L., Cotsarelis, G., … Brown, E. J. (2007). Deletion of the Developmentally Essential Gene ATR in

Adult Mice Leads to Age-Related Phenotypes and Stem Cell Loss. Cell Stem Cell, 1(1), 113–126. https://doi.org/10.1016/j.stem.2007.03.002

Sahin, U., Türeci, O., Schmitt, H., Cochlovius, B., Johannes, T., Schmits, R., … Pfreundschuh, M. (1995). Human neoplasms elicit multiple specific immune responses in the autologous host. Proceedings of the National Academy of Sciences of the United States of America, 92(25), 11810–11813.

Sakuishi, K., Apetoh, L., Sullivan, J. M., Blazar, B. R., Kuchroo, V. K., & Anderson, A. C. (2010). Targeting Tim-3 and PD-1 pathways to reverse T-cell exhaustion and restore anti-tumor immunity. The Journal of Experimental Medicine, 207(10), 2187–2194. https://doi.org/10.1084/jem.20100643

Shankaran, V., Ikeda, H., Bruce, A. T., White, J. M., Swanson, P. E., Old, L. J., & Schreiber, R. D. (2001). IFNγ and lymphocytes prevent primary tumour development and shape tumour immunogenicity. Nature, 410(6832), 1107–1111. https://doi.org/10.1038/35074122

Selby, M. J., Engelhardt, J. J., Johnston, R. J., Lu, L.-S., Han, M., Thudium, K., … Korman, A. J. (2016). Preclinical Development of Ipilimumab and Nivolumab Combination Immunotherapy: Mouse Tumor Models, In Vitro Functional Studies, and Cynomolgus Macaque Toxicology. PLoS ONE, 11(9). https://doi.org/10.1371/journal.pone.0161779

Smith-Garvin, J. E., Koretzky, G. A., & Jordan, M. S. (2009). T Cell Activation. Annual Review of Immunology, 27, 591–619. https://doi.org/10.1146/annurev.immunol.021908.132706

Swart, M., Verbrugge, I., & Beltman, J. B. (2016). Combination Approaches with Immune-Checkpoint Blockade in Cancer Therapy. Frontiers in Oncology, 6. https://doi.org/10.3389/fonc.2016.00233

Stutman, O. (1974). Tumor Development after 3-Methylcholanthrene in Immunologically Deficient Athymic-Nude Mice. Science, 183(4124), 534–536.https://doi.org/10.1126/science.183.4124.534

Stutman, O. (1979). Chemical Carcinogenesis in Nude Mice: Comparison Between Nude Mice From Homozygous Matings and Heterozygous Matings and Effect of Age and Carcinogen Dose. JNCI: Journal of the National Cancer Institute, 62(2), 353–358. https://doi.org/10.1093/jnci/62.2.353

Tang, H., Wang, Y., Chlewicki, L. K., Zhang, Y., Guo, J., Liang, W., … Fu, Y.-X. (2016). Facilitating T cell infiltration in tumor microenvironment overcomes resistance to PD-L1 blockade. Cancer Cell, 29(3), 285–296. https://doi.org/10.1016/j.ccell.2016.02.004

Taube JM, Anders RA, Young GD, et al. Colocalization of Inflammatory Response with B7-H1 Expression in Human Melanocytic Lesions Supports an Adaptive

Resistance Mechanism of Immune Escape. Science translational medicine. 2012;4(127):127ra37. http://doi.org/10.1126/scitranslmed.3003689

Verhoeyen, E., Costa, C., & Cosset, F.-L. (2009). Lentiviral Vector Gene Transfer into Human T Cells. In Genetic Modification of Hematopoietic Stem Cells (pp. 97–114). Humana Press. https://doi.org/10.1007/978-1-59745-409-4_8

Xu, Y., Zhang, M., Ramos, C. A., Durett, A., Liu, E., Dakhova, O., … Dotti, G. (2014). Closely related T-memory stem cells correlate with*in vivo* expansion of CAR.CD19-T cells and are preserved by IL-7 and IL-15. Blood, 123(24), 3750–3759. https://doi.org/10.1182/blood-2014-01-552174

Yong, C. S. M., Dardalhon, V., Devaud, C., Taylor, N., Darcy, P. K., & Kershaw, M. H. (2017). CAR T-cell therapy of solid tumors. Immunology and Cell Biology, 95(4), 356–363. https://doi.org/10.1038/icb.2016.128

Wang, T., Wei, J. J., Sabatini, D. M., & Lander, E. S. (2014). Genetic Screens in Human Cells Using the CRISPR-Cas9 System. Science, 343(6166), 80–84. https://doi.org/10.1126/science.1246981

Wiede, F., Gruta, N. L. L., & Tiganis, T. (2014). *PTPN2* attenuates T-cell lymphopenia-induced proliferation. Nature Communications, 5, 3073. https://doi.org/10.1038/ncomms4073

Wong, A. S. L., Choi, G. C. G., Cui, C. H., Pregernig, G., Milani, P., Adam, M., … Lu, T. K. (2016). Multiplexed barcoded CRISPR-Cas9 screening enabled by CombiGEM. Proceedings of the National Academy of Sciences, 113(9), 2544–2549. https://doi.org/10.1073/pnas.1517883113

Curran, M. A., Montalvo, W., Yagita, H., & Allison, J. P. (2010). PD-1 and CTLA-4 combination blockade expands infiltrating T cells and reduces regulatory T and myeloid cells within B16 melanoma tumors. Proceedings of the National Academy of Sciences of the United States of America, 107(9), 4275–4280. https://doi.org/10.1073/pnas.0915174107

Zarour, H. M. (2016). Reversing T-cell Dysfunction and Exhaustion in Cancer. Clinical Cancer Research : An Official Journal of the American Association for Cancer Research, 22(8), 1856–1864. https://doi.org/10.1158/1078-0432.CCR-15-1849

Zhou, P., Shaffer, D. R., Arias, D. A. A., Nakazaki, Y., Pos, W., Torres, A. J., … Wucherpfennig, K. W. (2014).*in vivo* Discovery of Immunotherapy Targets in the Tumor Microenvironment. Nature, 506(7486), 52–57. https://doi.org/10.1038/nature12988